MODEL ADHESIVE STUDIES USING BLOCK COPOLYMERS

by

Anne Booth Wood

Thesis submitted to the Faculty of the

Virginia Polytechnic Institute and State University

in partial fulfillment of the requirements for the degree of

MASTER OF SCIENCE

in

Chemistry

APPROVED:

T. C. Ward, Chairman

J. E. McGrath

D. W. Dwight

June, 1982

Blacksburg, Virginia

To

My Parents

whose unfailing support provides the resources

and rewards for this work and

To

My Husband

who shares the promise of this and every

achievement

ACKNOWLEDGEMENTS

More gratifying than completion of these degree requirements has been the collaboration and friendship offered by faculty members, technicians, and fellow graduate students throughout the course of this work and beyond. It is with sincere thanks that they are listed here to acknowledge their active and interested participation in this thesis research: Dr. Madgy Iskandar, Pradip Das, Dan Sheehy, Randy Burrier, Dr. Jim Haw, Peggy Sheridan, and Chi Tran.

Thanks are extended to Drs. H. Hsieh, W. Wang and the Phillips Petroleum Company for kindly providing the adhesive samples. Special mention must be made of Emel Yilgor for conducting the thermal analysis; Carlile Price for electron microscopy; Dr. Donald Baird and Ramesh Pisipate for supervision of the rheological work; Fred Blair for exceptional and creative machine work to modify existing equipment; Debbie Farmer and Donna Perdue for typing and patient correction.

The author also acknowledges enlightening discussions with Dr. Garth Wilkes, Dr. J. E. McGrath, Dr. D. W. Dwight, and Dr. Halbert Brinson on various aspects of this work. Finally, appreciation for the research direction of Dr. Thomas C. Ward can only be understated. It is not without hesitation that this student leaves his professional and personable instruction. Her best wishes remain here for his future research efforts and the success of the newly founded Center for Adhesion Science and Techology.

This research was funded by the Army Research Office, Durham, under grant no. DAAG 29-80-K-0093.

TABLE OF CONTENTS

TABLE OF CONTENTS (Cont'd)

LIST OF TABLES

LIST OF FIGURES

LIST OF FIGURES (cont'd)

CHAPTER 1

INTRODUCTION AND LITERATURE REVIEW

The study of adhesive phenomena is simultaneously a diverse and specific endeavor. The quality of adhesive performance can seldom, if ever, be credited to a single property of an adhesive/adherend system; the diversity of possible adhesive/adherend pairings has created innumerable unique combinations of thermodynamic, kinetic, chemical, physical, mechanical, and rheological contributions to explain adhesion processes. Consequently, characterization of any adhesive system demands information from many disciplines including surface chemistry, rheology, mechanical testing, engineering mechanics, and fractography. The complex interrelationships among all these areas affecting joint performance is acknowledged throughout adhesion science. But as diversified as the approach to the study of any adhesive system must be, one recognizes, too, that the blend of these interrelationships differs from system to system. Obviously, the natures of the selected adhesive and adherend dictate which factors will predominantly govern the strength and durability of their composite joint. The uniqueness of every adhesive/adherend pair is the major obstacle to a universal theory of adhesion. Numerous models have been proposed to explain the nature of interfacial forces of attraction causing adhesion (1,2,3); however, most are qualified for particular kinds of substrates e.g. porous, polymer, and rigid (3). Despite these categories of adhesion theories there exist variables common to all systems, though certainly these variables may be

weighted differently for different systems. The multi-disciplined foundation for adhesion investigations suggests basic principles from which these common variables arise. In this review section, current concepts comprising disciplines pertinent to the study of any adhesive system are discussed. In addition, the contemporary theories of adhesion are summarized and the aforementioned common variables are highlighted for further consideration.

Surface Chemistry

Recent review articles on the science of adhesion devote considerable space to the combined topics of surface and interfacial aspects of adhesive systems (1,2,3). The foremost prerequisite to the adhesive joining of two materials is intimate molecular contact at their interface to maximize the contributing short range forces of attraction between molecules and to preclude the presence of air voids or foreign contaminants at the interface. The degree of this interfacial contact is described and predicted by the thermodynamically modeled concept of wetting. A liquid in contact with a solid surface is thermodynamically driven to an equilibrium state which minimizes the free energy of the system. There exist surface tension forces, $(\partial G/\partial A)_{p,T}$ where G=free energy and A=area, for each phase arising from the fact that the bulk solid and bulk liquid materials exert attractive dispersion (and sometimes Keesom) forces on molecules in their respective surface layers. These forces separate surface molecules beyond equilibrium distances such that work is required to return to the normal configuration. The relationship of

the various free energy or surface tension forces, γ, between interfaces is shown in Figure 1-1.

The contact angle, θ, is the only experimental parameter with which to quantify the wetting phenomenon. The Young equation, modified to account for equilibrium spreading pressure, π_s (the reduction of the surface tension of a solid due to adsorption of vapor on the solid), suggests both an indirect method for the measurement of the surface tension of a solid, γ_s, and a criterion for the spontaneous wetting of a solid substrate by a liquid. For spontaneous wetting to occur $\gamma_S > \gamma_{SL} + \gamma_{LV} + \pi_s$ ($\theta=0$). Obviously, a contact angle of zero implies that the liquid has spread over the substrate surface. This condition may or may not coincide with the process of complete wetting wherein every microvoid of the substrate topography is contacted by the spreading liquid.

Although contact angle measurements alone do not define surface tension values for solid substrates, Zisman's work propounding a relationship between cos θ and γ_{LV} for a series of liquids on a low-energy solid established the widely recognized critical surface tension concept of wetting. The critical surface tension of a solid, γ_c, is an extrapolated value of γ_{LV} at which cos $\theta=1$ (or $\theta=0$). Liquids whose surface tensions are below the critical surface tension value determined for a solid should wet that solid spontaneously. Sharpe and Schonhorn (4) have applied these ideas to the adhesion process and have proposed that γ_c of the adhesive must be less than that of substrate to achieve spontaneous spreading.

THE YOUNG-DUPRE EQUATION

$$\gamma_S = \gamma_{SL} + \gamma_{LV} \cos\theta + \pi_S$$

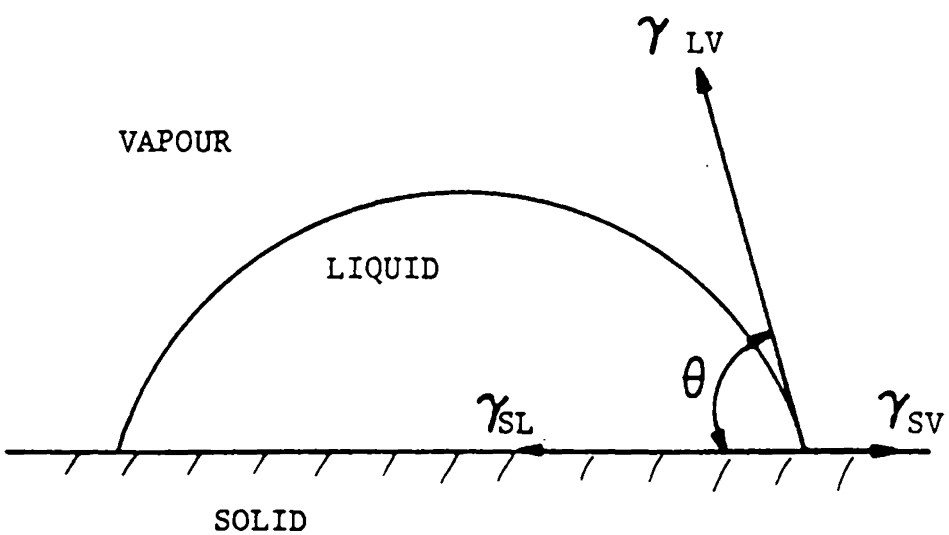

FIGURE 1-1. Surface free energy components for a liquid drop resting at equilibrium on a solid surface.

The Young equation and Zisman's critical surface tension concept of wetting were developed for advancing contact angles on smooth, energetically uniform model substrates. These assumptions are not realistic for most solids. The work of Johnson and Dettre on contact angle hysteresis is reviewed by Dwight and Riggs (55) as a more practical and informative technique for surface analysis from contact angle measurements. For energetically heterogeneous surfaces, advancing and receding contact angles encounter different energy barriers. The barrier to the advancing contact angle is low surface energy areas on the substrate. The barrier to the receding angle is high surface energy regions. The combined measurements of advancing and receding contact angles of test liquids on a solid provide information about the distribution of surface energies on that solid. The advancing contact angle is characteristic of the low energy portion of the solid surface, and the receding angle is characteristic of the high energy portion. Predominantly low energy surfaces show poor reproducibility of the receding contact angle. Scatter in data for advancing contact angles indicates predominantly high energy surfaces. The absence of contact angle hysteresis demonstrates a homogeneous surface.

Kinetic factors govern the wetting process as well and serve to emphasize additional considerations of surface chemistry in adhesion phenomena. Substrate topography plays a role in wetting processes as scratches, voids and other inhomogeneities may facilitate wetting through capillary draw action. Surface rugosity of a substrate will

also be cited later as contributing to mechanical interlocking and energy dissipation theories of adhesion mechanisms. Substrate surface area increased by rugosity could provide additional sites for maximized interfacial contact between adhesive and adherend or for contaminant adsorption. Studies by Wenzel (5) suggest that substrate roughness can modify contact angles either in favor of wetting or unfavorably depending on the system. Surface roughness can also cause contact angle hysteresis if rugosities are of the order of 0.5 μm or larger (55). Brewis and Briggs (6) state that the effect of surface topography on adhesion depends on surface energies, the viscosity of the wetting liquid, and the size and shape of irregularities. A variety of surface treatments provide means to selectively modify substrate energetics or microstructure, and eliminate impurities (6,7).

Kinloch (1) reviews a wetting mechanism in which the leading edge of a spreading film is followed by a region containing surface tension gradients imposed by thermal or concentration gradients in the liquid. The rate of flow in this region might exceed the rate of gravity flow in thick secondary film layers causing a ridge of liquid to develop. Concentration gradients in the spreading film of a liquid allude to the much debated weak boundary layer concept. For multicomponent materials, migration of the lowest surface energy constituent from the bulk to the interfacial region could result in a weak boundary layer in a composite joint. But generally this term applies to impurities, additives, or low molecular weight residues in polymeric adhesives.

Mill scale, rust or tarnish of a metallic substrate could also constitute a weak boundary layer. Bickerman (8) championed the premise that joint failure could never be interfacial but always occurred in cohesive failure of a weak boundary layer. His arguments were developed from probability theory applied to crack propagation in an adhesive joint.

Brewis and Briggs (6) summarize controversies surrounding the role of weak boundary layers in adhesion problems pertaining to polyethylene. They cite Bickerman's experimental evidence that polyethylenes reprecipitated to remove low molecular weight molecules demonstrated higher joint strengths than did the original polyethylenes. But independent workers (10) have denied the existence of weak boundary layers based on the same experiment for polyethylene using different substrates. Still others have developed a highly effective surface treatment for low surface energy polymer substrates based on the modification of weak boundary layers through irradiative crosslinking (9).

The influence of substrate topography and concentration gradients on the wetting process may be obscured as most adhesives are spread on their substrates by some applied force. Nevertheless, Bascom and Patrick (11) suggest that such effects may become important in the redistribution of adhesive after joint formation.

Dahlquist (21) defined a quantitative viscoelastic prerequisite for maximum molecular contact between mating materials. The Dahlquist criterion for establishing contact on a microscopic scale states that

the compressive tensile creep compliance (D) of the adhesive on a time scale approximating the bonding process (1 sec) must be greater than or equal to 10^{-7} cm^2/dyne. If $D(1) < 10^{-7}$ cm^2/dyne, the adhesive is "contact limited" and loses tack. Kraus, et al. (45) applied the Dahlquist criterion to linear and radial triblock copolymer adhesives of styrene with butadiene or isoprene. The criterion requires a high diene block molecular weight, specifically a diene continuous phase material, because connected polystyrene domains decrease the compliance of the adhesive in the time frame of bond-forming processes.

Although there is some debate (1) as to the importance of complete wetting to the adhesion process, it remains the basis for the most widely accepted adhesion theory today.

Rheology and Mechanical Properties

The function of an adhesive in a joint assembly is to transfer loads through tension and shear between mating surfaces. Thus the responses of both adhesive and adherend materials to these loads govern to a large degree the performance of an adhesive bond. Their responses are defined by the mechanical and rheological parameters such as elastic moduli, viscoelastic response, and the ultimate properties.

Determinations of elastic moduli and stress-strain behaviors are specific to particular mechanical tests which are reviewed by Nielsen (12). However, shear moduli and melt viscosity measurements can be made using a variety of dynamic mechanical testing techniques.

Rheological information on the melt of a polymer adhesive can also be obtained using different operational modes of a single rheometer. Thus, one must specify a melt viscosity measurement as arising from a capillary viscometer, a steady-state cone and plate rheometer, or from the dynamic or oscillatory rheometer employing either a cone and plate or parallel plate mode. For multicomponent systems including some block copolymers, different values for the melt viscosity of one type of sample may be obtained by different rheometers (13,30) indicating distinctive rheological (morphological) states of the polymer melt which depend on the method of measurement. Comparison of the dynamic mechanical and rheological properties of adhesives also interjects the factors of the shear rate and stress amplitude dependences of these properties. This spectrum of dynamic testing parameters ultimately raises questions about which testing mode and testing frequencies best approximate the service and application conditions of the adhesive being studied. Although dynamic oscillatory testing offers the most information about molecular structure/property correlation for characterization of a polymeric adhesive, there is a possibility, particularly for some block copolymer systems, that the rheological quantities defined in this way are not the same as those operating under the conditions of joint formation or fracture.

Nielsen (14) offers a concise introduction to oscillatory rheometers. The dynamic mechanical results are generally given in terms of complex numbers. The shear modulus, shear compliance, and complex viscosity, as well as the tensile modulus, are composed of a

real term and an imaginary term related to energies stored or dissipated during deformation. Table 1-1 summarizes the complex parameters, their component terms, and their interrelationships.

A few applications of the quantities in Table 1-1 to adhesion problems are given below. Tensile and shear moduli appear in expressions derived to quantitate the inherent stresses in a composite joint arising from thermal and mechanical aspects of joint formation (3,15). The importance of the melt viscosity of the adhesive can be viewed in context of wetting. The surface free energy criterion for wetting applies only for systems of negligible viscosity. For other systems the flow of the polymeric adhesive becomes a kinetically controlled process. Viscosity controls the spreading rate, the shear compliance if the adhesive is forcibly spread, and, hence, the extent of interfacial contact for joint formation.

The contributions of these same compliances, moduli and viscosities to practical adhesion is also noted. If one assumes that a good adhesive bond has been formed, that is, free of weak boundary layers and with interfacial forces exceeding cohesive forces, then failure of the joint should occur in the bulk adhesive and the mechanical and rheological properties of the bulk will dictate the fracture mechanism. For example, Gent and Hamed (16) studied the relative adhesive strengths of a styrene-butadiene random copolymer and a styrene-butadiene-styrene triblock copolymer on poly(ethylene terephthalate). Assuming surface energetics were comparable, the superior adhesive strength of the triblock copolymer was attributed

TABLE 1-1

Complex Quantities in Dynamic Mechanical Testing

Complex Quantity	Components	Type of Energy Term	Related by
Viscosity η^*	dynamic viscosity η' imaginary viscosity η''	loss storage	$\eta^*=\eta'-i\eta''$
Shear Modulus G^*	dynamic modulus G' loss modulus G''	storage loss	$G^*=G'+iG''$
Shear Compliance J^*	storage compliance J' loss compliance J''	storage loss	$J^*=J'-iJ''$
Tensile Modulus E^*	elastic modulus E' loss modulus E''	storage loss	$E^*=E'+iE''$
Tensile Compliance	storage compliance D' loss compliance D''	storage loss	$D^*=D'-iD''$

Equations of Interest

$G'=\omega\eta'' = J'/J^2$ ω=frequency of oscillations in rad/sec

$G''=\omega\eta'$ $J'=G'/G^2$ $G^2=(G')^2+(G'')^2$

to differences in the dissipative properties of the random and triblock copolymer materials.

Joint Design and Stress Analysis

Joint geometry and joint dimensions exert a dramatic influence on adhesive bond strength and efficiency. Ryder and Shields (3,17) catalog numerous recommended joint configurations which demonstrate both classic and novel combinations of the four basic joint types: angle, tee, butt, and parallel surface. Each configuration is designed to support one or more of the four stresses or loadings outlined below:

1) Shear imposes an even stress across the whole bonded area and thus uses the joint area most efficiently,
2) Tension also imposes an evenly distributed stress unless adherends are flexible under the applied load,
3) Cleavage results from an offset tensile force or moment. Stress is not evenly distributed but is concentrated at one side of the joint,
4) Peel places very high stress on the boundary line of the joint. One or both adherends must be flexible.

Because there exist many joint configurations suitable for each type of loading, joint design for most applications becomes a decision of ease of manufacture, cost, and taste. Shear loading, specifically the lap shear joint, is the most practical and efficient way of adhesive bonding, and is also simple and economical to prepare. The lap shear joint was selected for the test program described in this

thesis. Therefore, the remainder of this discussion will be devoted to the stress and dimensional analyses of the simple lap shear joint.

Bickerman (8) makes a pictorial case for the similarity of the adhesive-air boundary in a lap joint to a square hole or flaw in a two dimensional film. Bickerman assumes that the adherends are not flexible and employs the mathematical treatment by Savin to quantify the stress concentration parameter β. The value of β is derived from the ratio of adhesive thickness to adherend thickness and is calculated for Bickerman's example to be equal to 6. This means that the maximum stress on the adhesive at the edges of the lap joint is actually six times the average stress. Figure 1-2 represents the shear stress distribution in a lap shear specimen.

Anderson, et al. and Ryder (18,3) offer other sample calculations of maximum adhesive shear stress and maximum adhesive tensile stress for a simple lap joint. The equations involve factors like bond length, adhesive and adherend thickness and moduli, and Poisson's ratio for the adherends. While these expressions are still "ultraconservative approximations" (3) of the true reaction of these joints under uniaxial loading, they do provide relative predictions of the effects of the changes in geometry or materials on the lap joint.

Anderson, Bennett and DeVries (18) summarize the history of theoretical stress analyses of lap joints. Beginning with considerations by Volkersen of only the differential strains in lap joints, others extended the treatment to include the deformation of the adherends and the transverse strains in the adhesive associated

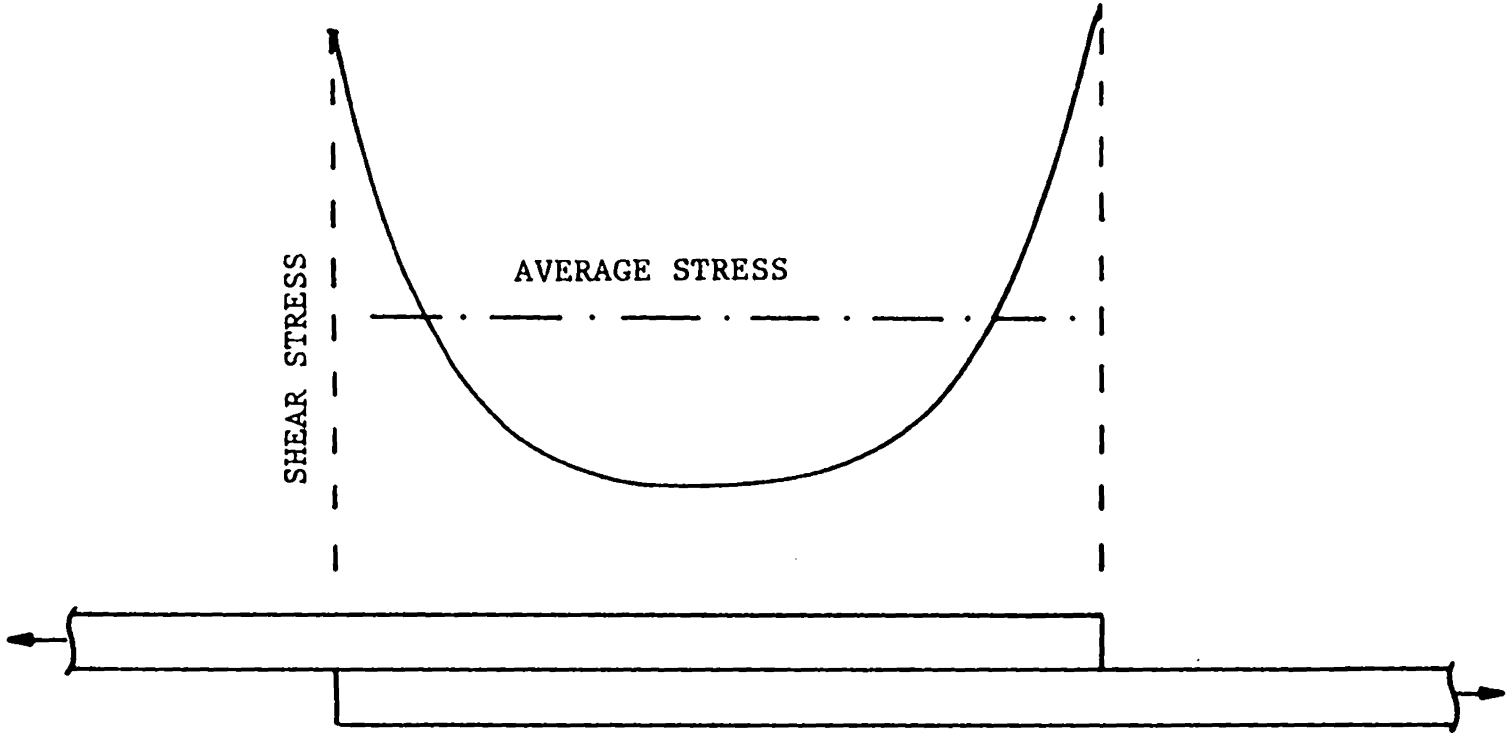

FIGURE 1-2. Shear stress distribution in a simple lap shear joint.

with tearing stresses. A sample calculation using the Goland-Reissner stress analysis demonstrates the mathematical rigor of available methods to quantify the internal stresses of lap specimens under load (18). Recently Delale and Erdogan (46) formulated a thorough mathematical analysis for the stress distributions in a model viscoelastic adhesive under membrane loading, bending, and transverse shear loading of a single lap joint. Joint dimensions were generalized in this treatment. Greenwood (15) has summarized the stress concentration factor approach to lap joint strength analysis for various adherend and adhesive rigidities.

Stress distribution is greatly affected by the relative flexibility of the adhesive and the adherend. Recalling the nonuniform stress distribution of a typical lap joint (Figure 1-2), it is not surprising that joint strength is not a linear function of lap length. The area of the bond which carries comparatively low stress is the area adjacent to the center of the lap. Increasing the width of the joint gives a proportional increase in strength. Increasing the overlap length beyond a certain limit has little effect (17). The correlation between joint dimensions and shear strength is generally represented by plots of failure stress vs. ℓ/t where ℓ = overlap length and t = adherend thickness.

The thickness of the adhesive layer also affects joint strength (3,16). For most systems there exists an optimum bondline thickness which depends on the loading mode, adherend species, joint design, and test temperature. A suitable thickness in most cases of structural

bonding of metals employing shear loading falls in the range of 0.08 to 0.13 mm (3 to 5 mils). The American Society for Testing Materials (ASTM) specifies other recommended dimensions for lap shear preparation (18).

Other categories of stress origin in adhesive joints besides those related to their mechanical construction are thermal stresses resulting from different coefficients of thermal expansion in the adhesive and adherend. Bickerman (8) discusses several examples of such "shrinkage stresses," particularly as they relate to coating systems and various environmental conditions to which joints are subjected.

Although little can be done to eliminate all the stress contributions to joint failure, preparative methods should be honed to ensure the absence of local stress raisers such as inclusions or air voids, while tension in joint edges due to asymmetric loading must be conscienciously minimized.

Engineering Mechanics

A common goal of the many failure tests devised to measure the strength of adhesive bonds is quantitation of the forces that constitute breaking criteria. Before the recognition of the importance of inherent flaws in materials, the analyst relied on average stress or strain data: maximum tensile stress or maximum principle strain which statistically reflected the presence and distribution of microvoids. Associated with the stress-strain approach, a total fracture energy derived from the intergral of the stress-strain curve for a composite joint was frequently reported.

Although some workers (19) even propose a graphical division of this total fracture energy into elastic and nonelastic energy contributions, the total fracture energy defined from stress-strain integrals affords no mechanistic information that might distinguish interfacial (bond-making) or practical (bond-breaking) energy components of the adhesion process.

An insightful summary of the continuum fracture mechanics approach to fracture analysis is presented in a recent book by Anderson, Bennett, and DeVries (18). When the inherent flaws in one of the component materials of an adhesive joint are larger than the average flaw size distribution and are relatively sharp, former methods of analysis using stress concentration factors at the crack tip prove theoretically impractical. Griffith was the first to circumvent this problem by considering the changes in strain energy during failure processes in brittle materials. His work created the concept of a critical applied stress at which the strain energy of deformation of the fracture area just equals the work required to create a new fracture surface. That is, for a crack of length 2a, given that the elastic strain energy of deformation, U, equals $\frac{\pi a^2\sigma^2}{E}$ where E is Young's modulus for the material, then the crack propagation condition is

$$\frac{\partial}{\partial A}\left[\frac{\pi a^2\sigma^2}{E}\right] > \frac{\partial}{\partial A}(4aT)$$

where T is the surface tension. The critical applied stress, σ_{cr}, is

then $\left[\frac{2ET}{\pi a}\right]^{1/2}$.

The extension of the Griffith theory to systems in which plastic energy dissipation accompanies crack growth requires additional terms in an energy balance equation. Irwin and Orowan's (44) modified Griffith equation states that $\partial W + \partial U \geq \partial T + \partial \Psi = \partial \Gamma$, where

∂W = the change in external work during crack growth, ∂A,

∂T = increase in surface energy,

∂U = elastic strain energy,

$\partial \Psi$ = plastic flow energy dissipation in crack growth,

$\partial \Gamma$ = fracture energy.

(For metals, plastics, and most other non-brittle materials $\partial \Psi >> \partial T$.) This theory defines a specific fracture energy, G_c, sometimes called the critical energy release rate such that $\partial \Gamma = G_c \partial A$. G_c is assumed to be a material property and has the dimensions energy per unit area.

Although the Griffith theory originated for the case of cohesive failure, the same arguments are applied to adhesive fracture, in which case ∂T can be equated to the work of adhesion which is still much less than $\partial \Psi$ for viscoleastic materials. The form of the modified Griffith equation for a critical applied stress for an adhesive bond is complicated by the inclusion of geometric and stress-intensity factors. However, the energy balance equation applies directly and G_c, defined in the same way, is renamed the adhesive fracture energy. Because surface preparations can affect G_c, the adhesive fracture energy is not strictly a material property, but it nevertheless

provides a powerful system parameter (and a theoretically founded one) for predicting adhesive failure.

The fracture mechanics analysis has been adopted as a most meaningful treatment for the universal interpretation of failure testing data. A recent paper by Gent (20) reviews equations relating breaking stress and adhesive fracture energy for the commonly employed peel and lap shear tests. A chapter of the aforementioned text by Anderson (18) is devoted to the complete and rigorous stress analysis and fracture mechanics treatment of the lap shear joint, the peel test, the cone test, the blister test, and the widely acclaimed cantilever beam test. The latter employs a design geometry by Mostovoy and Ripling (43) to yield G values independent of crack length.

Fracture Phenomena

Characterization of joint failure after fracture provides the essential determination of the failure locus. Some possibilities for this locus include: (1) purely interfacial failure, (2) cohesive failure of the adhesive, (3) cohesive failure of an oxide layer on a metal substrate, (4) cohesive failure of a primer layer (if present), or (5) interfacial failure between the adhesive and primer layers, or combinations of all these failure modes. The locus of failure can inform the investigator about the relative strengths of interfaces and mating materials; however, the failure locus may depend on testing rates, the load types, and aging effects. Smith and Kaelble (7) have analyzed the total bond strength of an epoxy phenolic adhesive on Al

and Ti alloys in terms of the relative proportions of interfacial and cohesive failure. The aging of these metal substrates and of their joints in humid environments has also been studied in terms of its effect on the total bond strength and the percent of cohesive failure for the systems. Exposure of the Al substrate to higher relative humidities caused surface degradation (oxide growth and contamination), a decreased fraction of cohesive failure (ϕ_c) and lower total bond strengths (σ_b). A linear relationship was observed between ϕ_c and σ_b. Surface aging of phosphate-fluoride treated Ti 6-4 in humidity chambers produced negligible change in oxide thickness, bond strength, or fraction of interfacial failure. For both substrates joint exposure in a humidity chamber caused degradation of the adhesive (not the interface) and reduced bond strength.

Bird and colleagues (22) first cited the need for systematic electron micrography of fracture surfaces. In this initial work, flexurally fractured polystyrene and a polystyrene-acrylonitrile copolymer were examined. The fracture surfaces of polystyrenes have since received considerable attention (22,23,24) owing to their characteristic display of fibers associated with the regions of surface deformation. Several mechanisms for the fiber formation have been hypothesized in these independent studies. Regardless of mechanism the fiber formation is thought to increase the stress-bearing capacity of a polystyrene adhesive bond and to provide a means of energy dissipation that contributes to high adhesive bond strengths.

Theories of Adhesion

As stated previously the uniqueness of every adhesive/adherend pair is the major obstacle to a universal theory of adhesion. Furthermore, such a theory must address the phenomenological duality of an adhesive bond, that is, the separate and irreversible mechanisms of interfacial attraction and joint failure which rarely occurs exclusively at the interface. Joint failure conditions (e.g. testing speed, geometry) can themselves determine the strength of an adhesive bond regardless of the inherent chemistry at the interface. These two separate phenomena are frequently referred to as interfacial (bond-making) and practical (bond-breaking) adhesion. It is not suprising, then, that current theories of adhesion fall into these same categories.

The most generally accepted theory of interfacial adhesion has not been weakened by the development of alternative postulates. The wetting or contact theory of adhesion, also known as the adsorption theory, states that interfacial strengths based on van der Waals forces of attraction alone are sufficient to exceed the measured joint strength of most materials chosen for adhesive assembly. Calculations have been performed to support this hypothesis (1). Discrepancies between calculated and actual joint strength are attributed to defects and stress raisers present in every joint.

Intrinsic interfacial adhesion is ascribed by other theories to 1) mechanical keying or interlocking of the adhesive into the substrate surface, 2) interdiffusion of polymeric adhesive and

polymeric adherend molecules to form an interlaced network, 3) electrostatic forces created by an electrical double layer when dissimilar materials are in close proximity, 4) chemical reaction and the formation of primary valence bonds between adhesive and adherend. Although there are systems for which each of these mechanisms has been shown to contribute to the intrinsic adhesive forces (1), each theory is only advanced for certain classes of adhesive systems, i.e. mechanical interlocking is now though to be a factor only in the joining of porous or fibrous surfaces, interdiffusion only for mutually soluble polymer systems, and so on. Moreover, these alternative theories still require the molecular contact of the wetting theory, and thus interfacial adhesion via van der Waals forces is also established.

In response to aspects of practical adhesion the mechanical deformation or rheological theory states that the strength of adhesive joints in the absence of weak boundary layers is determined by the mechanical deformation properties of both the adhesive and adherend and by local stresses in the joint. Similarly, the fracture theory of adhesion attributes discrepancies between ideal and actual joint (adhesive) strength to the irreversible processes of joint fracture (viscoelastic energy dissipation) and the defects present in interfacial and bulk phases. Embracing the Griffith-Irwin parameters, the fracture theory equates fracture energy to a sum of the work of adhesion, defined by the surface energies of the system, and the total work for the irreversible fracture processes. It is the magnitude of

this second term that obscures the work of adhesion and dominates the value of the fracture energy primarily because it seems impossible to know exactly what are the true stresses in a failing joint.

A description of adhesion which incorporates aspects of interfacial and practical adhesion theory is one that distinguishes stages of adhesive bond formation. Interfacial contact by wetting is the primary step. Adhesive strength can then be enhanced in a second stage involving processes like interdiffusion or chemical bonding. Ultimately, the mechanical strength of the adhesive bond will be determined by the extent of wetting, the size of defects, and the extent of irreversible deformation in the fracture zone as a function of the viscoelasticity of the bulk phases.

The Dominant Variables

Kaelble (25) groups the prominent factors influencing joint strength into the interfacial factors which reiterate various adhesion theories and the system factors which summarize the mechanical considerations of joint construction. His list is reproduced in Table 1-2. If one concedes that cosolubility for interdiffusion, chemical bonding, electrostatic effects, etc. are special contributions for some systems, this list can be condensed to seven general variables for any adhesive system. These variables, which will be labeled the "dominant variables" governing adhesive processes and performance, are

1) Adherend nature and topography
2) Adherend and adhesive contamination
3) Wetting

Table 1-2

Prominent Factors Influencing Joint Strength

A. Interfacial factors

1. Dispersion-polar interactions
2. Adherend wettability
3. Adhesive-adherend cosolubility
4. Surface adsorption layers
5. Weak boundary layers
6. Chemical bonding
7. Special electrostatic effects

B. System factors

1. Geometry of loading
2. Joint design
3. Adhesive rheology
4. Adherend rheology
5. Residual stresses
6. Load induced stress concentrations

4) Residual stresses

5) Mechanical properties of adhesive and adherend

6) Rheology of adhesive and adherend

7) Aging

Statement of the Problem and Objective

The emphasis in present industrial technology on high performance adhesives has led to an even more complicated puzzle of adhesive modeling. In addition to the aforementioned dominant variables for these systems, primer solutions, solvent contamination and entrapment, nonroutine cure pressures and temperatures, and other procedural artifacts further obscure the fundamental contributions to adhesion of the polymer adhesive itself.

In this work use of an "homologous series" of block copolymers as hot-melt adhesives simplifies the number of components involved in the adhesive bond formation while providing a systematic gradation of properties through which to assess the relative contributions of viscoelastic, morphological, and surface energy parameters. The series employed is a styrene-isoprene-styrene (SIS) linear triblock system, the samples having narrow molecular weight distributions and ranging in styrene content from 20 to 60 percent by weight. The objective of the study is to control the set of dominant variables in terms of equalizing their contributions to each copolymer adhesive system. Such control would serve to eliminate the variation of these factors among the different adhesive systems in order to unravel more

fundamental distinctions between adhesives that are usually obscured by the effects of the dominant variables.

The Thermoplastic Elastomers

The styrene-isoprene-styrene (SIS) triblock copolymers used as model hot-melt adhesives in this study were selected because of the abundant knowledge available on the characterization of such thermoplastic elastomers. This class of materials was introduced commercially by Shell in 1965 and is defined by an ordered block copolymer composition, ABA, where A represents a block which is glassy or crystalline at service temperatures but fluid at higher temperatures, and B is a block which is elastomeric at service temperatures. The best-known commercial materials are the styrene-diene-styrene type. The thermodynamic incompatibility of the blocks creates a two-phase morphology in which the relative volume fractions of the two components govern the shape of discrete or semicontinuous domains of the glassy phase in the elastomeric matrix. Kaelble (25) argues geometrically that spherical domains of styrene in a simple cubic lattice arrangement will begin to coalesce to cylinders at styrene volume fractions of 30%. A change from cylindrical microdomains to lamellae is expected when the volume fractions of styrene and diene are approximately equal. Because the two ends of every elastomeric chain are chemically linked or anchored in a glassy domain, the effect of physical crosslinking imparts high performance properties to these materials - high resilience, high tensile strength, highly reversible elongation, and abrasion resistance - without chemical vulcanization.

The elastomeric performance of ABA copolymers depends on the block lengths and weight fractions of A and B components. The (now) classical anionic polymerization methods for these materials reviewed by McGrath (26) provide the required control of block length and molecular weight distribution essential to the structure-property correlations.

Mechanical properties of styrene-diene-styrene triblock systems exhibit a range of behaviors depending upon the proportion of segmental styrene. Stress-strain curves vary from those typical of a conventional vulcanizate for low styrene content, to ductile behavior at intermediate styrene percentages, to brittle fracture at highest styrene contents. Tensile modulus and hardness values increase gradually with increasing percent styrene up to values typical of pure polystyrene. For a constant proportion of styrene these mechanical properties remain virtually unaffected by changes in overall molecular weight.

Several theories have been put forth to explain the enhancement of tensile strength of the elastomeric networks of ABA copolymers. These theories are briefly reviewed by Holden, et al.(13). Essential to the arguments are the concepts of stress redistribution and energy absorption by domains acting as filler particles and by allowable slippage of chain segments between chain entanglement crosslinks. Kaelble (25) also presents the series-parallel model of response to define the tensile moduli of these materials as a mathematical function of the moduli of the homopolymers acting in combined series and parallel arrangement.

The flow behavior of the ABA block copolymers is quite complex due to the nature of the two-phase system. Enhanced viscosities over those for corresponding random copolymers or homopolymers are attributed to the additional energy required to move polystyrene through the incompatible diene matrix. Dynamic viscosities and dynamic moduli of the SBS (B=butadiene) and SIS systems exhibit temperature, molecular weight and frequency dependences. Most workers report non-Newtonian behavior of these quantities for the copolymers at low shear rates (27,29,30,38,39,40). The nature and onset temperature of a flow transition from non-Newtonian to Newtonian behavior of both dynamic viscosities and moduli have been in question (27,28,30). There is increasing evidence that this transition is related to the integrity of the two-phase system under test temperatures and frequencies (30,41). Disruption or dissolution of the domain structure is favored by high strain levels, low frequencies, and high temperatures. Also, above the transition temperature agreement between dynamic and steady state viscosities for SBS (30) implies the absence of domain morphology.

Adhesive Properties of SIS Copolymers

The literature on adhesive properties of SIS block copolymers will be confined to the reported papers of J. M. Widmaier and G. C. Meyer who have investigated the relationship of mechanical, rheological, and optical properties of various SIS block copolymers to their adhesive shear strengths. Because of the transparency of SIS films, Widmaier and Meyer elected to study their hot-melt adhesive performance with vapor degreased glass substrates. Under these

workers' conditions of lap joint formation and fracture the following results were obtained (33):

1. Cohesive failure was observed when the isoprene content of the adhesive was less than or equal to 50% of the total copolymer $\overline{M}_n$. Above 50% isoprene content, joint failure was mostly interfacial. SIS compositions containing 50% isoprene displayed both types of failure.

2. Shear strength decreased with increasing molecular weight for constant percent isoprene content.

3. The highest shear strength (100 kg/cm^2) occurred for compositions of 30 mole percent isoprene and $20,000 < \overline{M}_n < 50,000$. This was attributed to the limited domain formation permitted by small component blocks of approximately equal length.

4. Shear strength of joints made from several copolymers of different percent isoprene content (molecular weights not reported) was dependent on the activation temperature of joint formation. For decreasing isoprene content maximum shear strength occurred at higher joint activation temperatures. The existence of a maximum in the plot of shear strength versus activation temperature was explained in terms of a corresponding isoviscous condition of the component blocks of the SIS material at the maximum shear strength activation temperature.

5. Aging of joints formed from a 29% isoprene-containing SIS ($\overline{M}_n$=31,000) at a constant temperature and humidity caused a loss in shear strength after 3 months followed by a progressive decline in adhesive strength. At the end of one year the adhesive retained 40% of the initial shear strength. It was suggested that stresses

induced by slow separation effects of the block phases could account for the reduced shear strength over time.

6. Star block copolymers prepared from the selected linear SI and SIS precursors possessing previously defined optimum molecular weight and relative block length parameters for adhesion showed improved shear strength over the linear SIS counterparts. For the same SIS precursor shear strength increased with the number of star branches. The improved adhesion was said to result from extended physical crosslinking of the adhesive through enlargement of the rigid styrene domains when they mix with the linking agent used in the synthesis of the star polymers. Also, the chemical junction points introduced in the linear SIS in star formation increased physical entanglements among macromolecular chains, thus improving cohesion within the star block copolymers (34).

Widmaier and Meyer's conclusions concerning the molecular parameters, M_{total} and percent isoprene, imparting optimal SIS adhesive properties are couched in a morphological argument. By precluding substantially ordered phase separation of the styrene and isoprene blocks, the adhesive morphology may be described as a statistical distribution of small isoprene nodules in a polystyrene matrix. This distribution favors superior contact with the substrate, good wetting, and therefore, good adhesion. The morphological argument was substantiated by optical (32) and rheological (29) characterization of various SIS materials possessing approximately 30% isoprene and the favorable and unfavorable molecular

weight ranges for adhesion. Transmission electron microscopy, optical polarized microscopy, and laser diffraction revealed isotropic films with random distributions of polyisoprene nodules for SIS samples of $M_{tot} < 35,000$. For $\bar{M}_n > 56,000$ the SIS films were anisotropic and showed a cylindrically structured morphology (32). Rheological characterization performed on a 38 weight percent isoprene SIS ($\bar{M}_n$ = 45,000) at temperatures ranging from 170-250°C verified a morphological transition around 215-225°C as evidenced by 1) a change from non-Newtonian to Newtonian behavior in the dynamic viscosity of the sample for low shear rates above 225°C, and 2) an abrupt change in the slope of the shear storage modulus vs. temperature plot at approximately 220°C. A statistical thermodynamic basis for this behavior attributed to phase miscibility was predicted by Leary and Williams (35). They defined a critical equilibrium temperature above the highest T_g of the copolymer for which the free energy of mixing is zero. The formation of an "interphase" region of mutually miscible block components has been experimentally suggested for other materials as well (28,36,37).

The nature of the interphase formation was explored by Widmaier and Meyer (29) using their intermediate molecular weight samples. (For higher MW samples, degradation would precede the critical equilibrium condition.) Optical polarized microscopy, small angle X-ray diffraction, and transmission electron microscopy/laser diffraction methods were employed to trace the morphological evolution of the SIS displaying different rheological properties at different temperatures. Small angle X-ray diffraction revealed a gradual and total loss of the

original lamellar structuring of the SIS sample with increased temperature.

Mechanical property data for SIS copolymers comprising a range of molecular weights and isoprene contents provided additional insight into their potential adhesive performance as detailed below (31):

1) The stress-strain behavior of thin (0.1mm) SIS films varied with isoprene content. For isoprene weight percents less than 40, films demonstrated elastic behavior with 2-5% elongation. For intermediate percent isoprene, films were characterized by ductile deformation to failure preceded by a yield point. Films with the highest isoprene contents demonstrated tensile elongation to the break point.

2) These different stress-strain behaviors were observed in both joint and film failure.

3) The elastic moduli did not depend significantly on molecular weight but decreased with increasing percent isoprene.

4) The average tensile strength (measured at the yield point when percent isoprene > 40) was a function of M_{total} and displayed a maximum value at different percent isoprene for a given M_{total} range. The maximum tensile strength corresponded to the calculated isoprene content and block molecular weight required for the onset of phase separation. Although the tensile strength would be expected to continue increasing as the proportion of the hard styrene phase increases, the relative decrease in the amount of isoprene restricts microphase separation and reduces thin film cohesiveness.

CHAPTER 2

EXPERIMENTAL

Materials

The Adhesives: Essentially monodisperse styrene-isoprene-styrene (SIS) linear triblock copolymers ranging in styrene content from 20 to 60 percent by weight were synthesized in approximately 35 g batches by Dr. Wayne Wang at the Phillips Petroleum Company. Table 2-1 summarizes the sample series by styrene content and block number average molecular weight. The dispersity ratios were provided by Phillips as determined by gel permeation chromatography. No evidence of homopolymer, diblock, or stabilizer additives could be seen in the chromatograms.

The Substrate: Coupons of titanium 6-4 alloy (6% aluminum, 4% vanadium) were provided by the NASA-Langley Research Center. The dimensions of each coupon were 2.54 cm x 12.7 cm x 0.127 cm (1" x 5" x 0.05"). Literature (7, 42) regarding various surface treatments and the subsequent aging characteristics of this titanium alloy stated that a strict adherence to the fairly standardized phosphate-fluoride surface treatment reported in Table 2-2 was essential for reproducible results. After air drying the cleaned coupons were immediately placed in "zip-lock" bags in a dessicator until needed for adhesive joint preparation.

Adhesive Film Preparation

Originally each neat copolymer powder was compression molded at

Table 2-1

Materials

Sample	Weight Percent Styrene	M_W/M_N (10^{-3})	S/I/S M_N (10^{-3})
A1	20	264/239	24/191/24
A2	21	229/209	22/165/22
A3	20	157/148	15/118/15
A4	20	229/209	22/165/22
B1	30	147/140	21/98/21
B2	33	145/135	22/90/22
B3	30	116/111	17/77/17
C1	40	114/109	22/65/22
C2	43	98/93	20/53/20
D1	50	96/92	23/46/23
D2	54	80/76	21/35/21
D3	50	65/63	16/31/16
E1	60	81/77	23/31/23
E2	59	64/61	18/25/18
E3	60	64/61	18/25/18
E4	60	59/57	17/23/17

Table 2-2

Phosphate-Fluoride Surface Treatment for Ti 6-4 Adherends*

1. Solvent wipe - methylethyl ketone
2. Alkaline clean - immerse in SPREX AN-9, 30.1 g/ℓ, 353 K (80°C) for 15 min
3. Rinse - deionized water at room temperature
4. Pickle - immerse for 2 min at room temperature in solution containing 350 g/ℓ of 70% nitric acid and 31 g/ℓ 48% HF.
5. Rinse - deionized water at room temperature
6. Phosphate/fluoride treatment - Soak for 2 min at room temperature in solution containing 50.3 g/ℓ of tri sodium phosphate (Na_3PO_4); 20.5 g/ℓ of potassium fluoride (KF); and 29.1 g/ℓ of 48% hydrofluoric acid (HF)
7. Rinse - deionized water at room temperature
8. Hot water soak - deionized water at 338 K (65°C) for 15 min
9. Final rinse - deionized water at room temperature
10. Dry - air at room temperature

*Ref. 42

150°C under 20,000 pounds pressure on a 3-5/8 inch diameter ram for 10 minutes. Reproducible cooling cycles were employed to reach approximately 65°C at which temperature the films were removed from the mold. The resulting film was 7.62 cm (3") in diameter and between 0.6 to 1 mm thick. From these films appropriate sample geometries were cut for mechanical property testing, wetting studies, rheological measurements, and for some adhesive joints.

A study of film contamination by different backing materials for compression molding was performed early in this work using X-ray Photoelectron Spectroscopy (XPS). Figures 2-1 and 2-2 show wide scan XPS spectra for adhesive films compression molded between Teflon and aluminum sheets respectively. Evidence of substantial contamination (15 atom percent fluorine) of the SIS adhesive film by Teflon (fluorine peaks at 692 eV, 684 eV, 651 eV, 632 eV, 606 eV) led to the use of aluminum backing for all compression molded films.

Neat polymer powder samples E2, D3, and C2 were prepared as oriented films for adhesive joints using a modified header and die for the Custom Scientific Instruments benchtop mixing extruder. All samples were extruded as films 1.9 cm (0.75") wide and 0.09 cm (35 mils) thick. Sample E2 was extruded at 170°C, D3 and C2 at 185°C; and all at the maximum rotor speed of 240 rpm. A commerical oriented styrene-butadiene-styrene, Kraton 2104, was supplied by the Shell Co. This material contained 30% styrene and was extruded at 170°C with a draw ratio of 4:1.

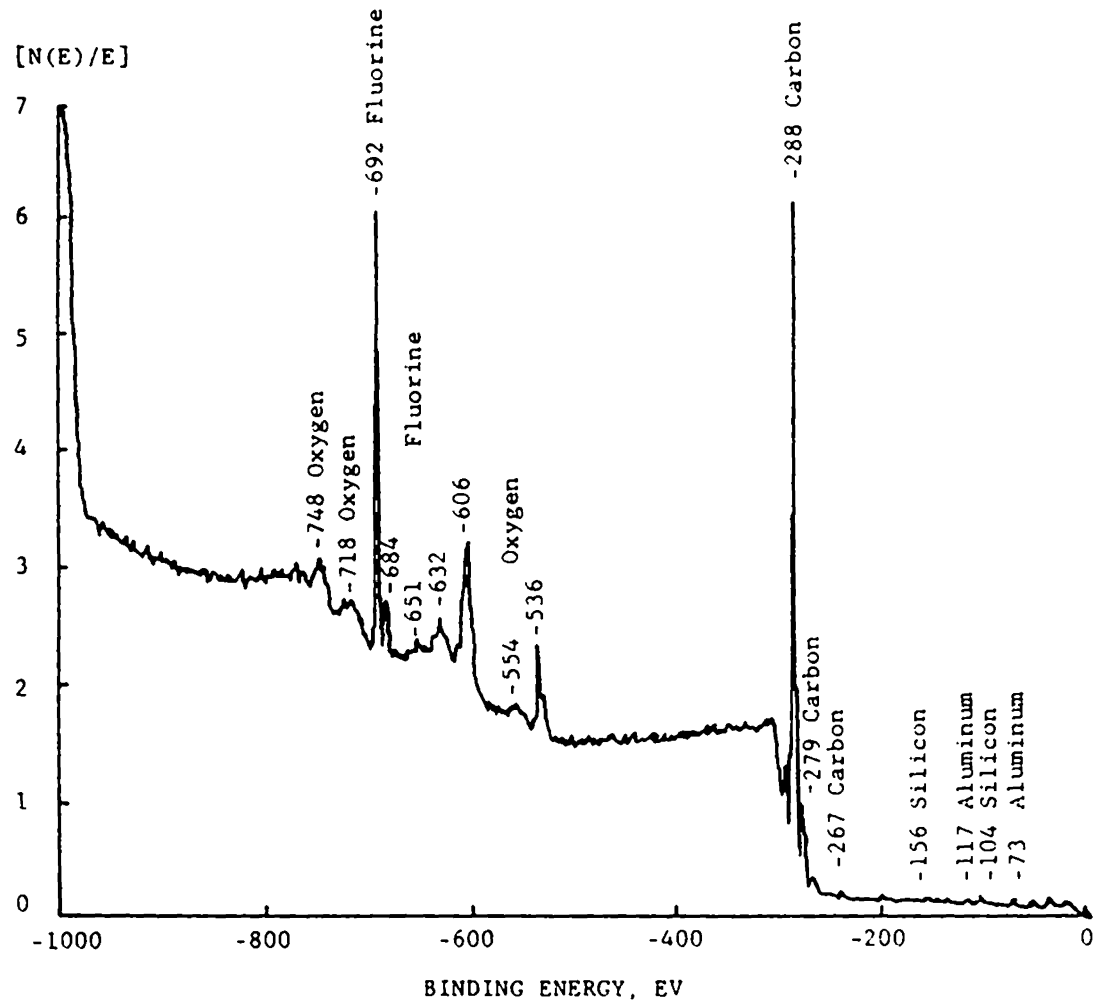

Figure 2-1. Wide scan XPS spectrum of E1 film compression molded between Teflon sheets

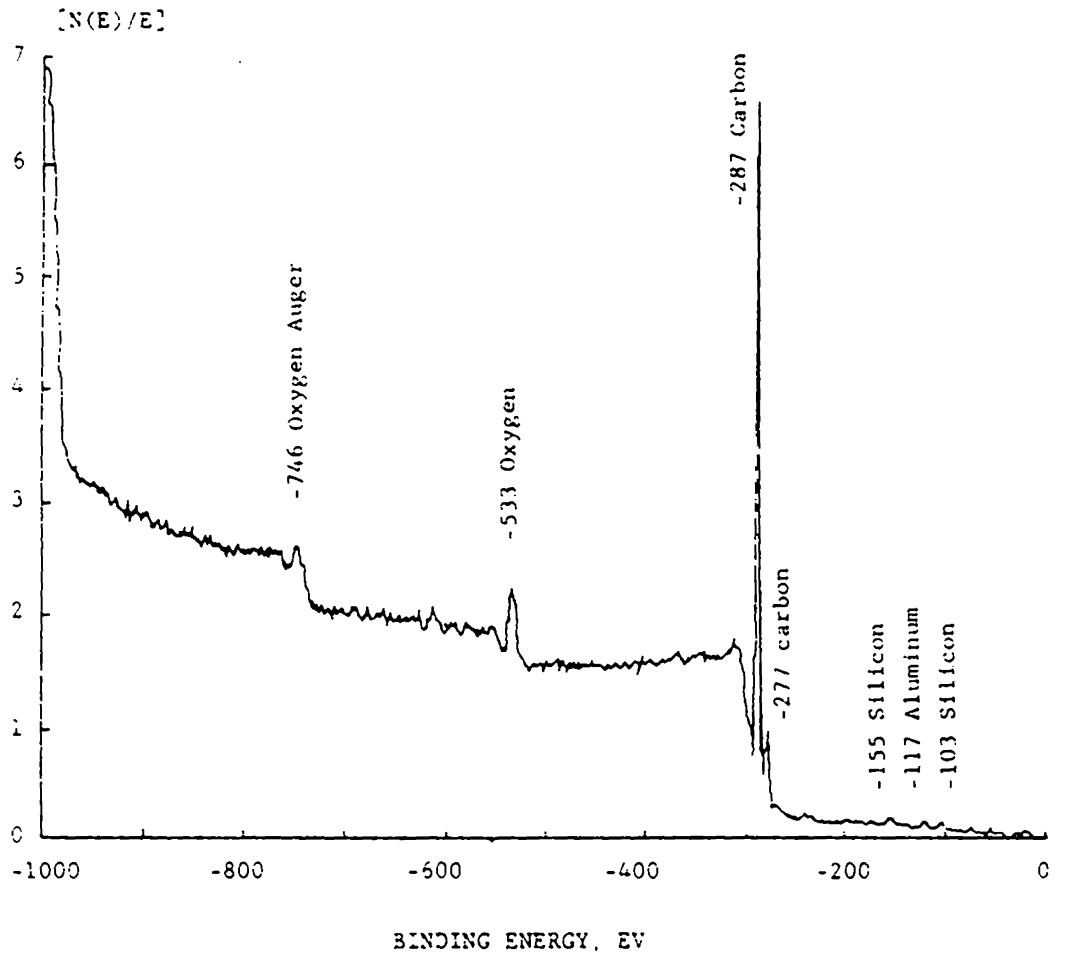

Figure 2-2. Wide scan XPS spectrum of E1 film compression molded between aluminum sheets

Joint Preparation

Single lap-shear joints with an overlap length of 1.27 cm (0.5"), bond area of 3.22 cm^2 (0.5 $inches^2$), and adhesive layer thickness averaging 0.38 mm were prepared. Pieces of adhesive film were cut from the compression molded or oriented films to match the bond area size. The lap joint was assembled in a specially designed gluing jig to prevent misalignment of the titanium alloy adherends. The gluing jig is pictured with mating adherends positioned in Figure 2-3. The entire jig assembly was pressed at a selected temperature (usually 150°C) at 20,000 pounds on a 3-5/8" diameter ram. Pressure was released after 10 minutes, and the joint remained at temperature for 3 additional minutes before cooling. The joints were cooled to 65°C, removed from the jig, trimmed of some excess adhesive, and stored in a dessicator until fracture.

Joint Fracture

All joints were fractured at room temperature between 24 and 48 hours after preparation on an Instron Table Model 1130 with a cross-head speed of 1 cm/min. Joint strength for each adhesive was measured as the maximum stress applied (the peak of the stress-strain curve), and the total fracture energy was obtained by integrating over the fracture curve on the Numonics Corporation Model 1224 Digitizer.

Wetting

A qualitative estimate of the ability of each adhesive to wet the phosphate-fluoride treated titanium alloy was made as follows:

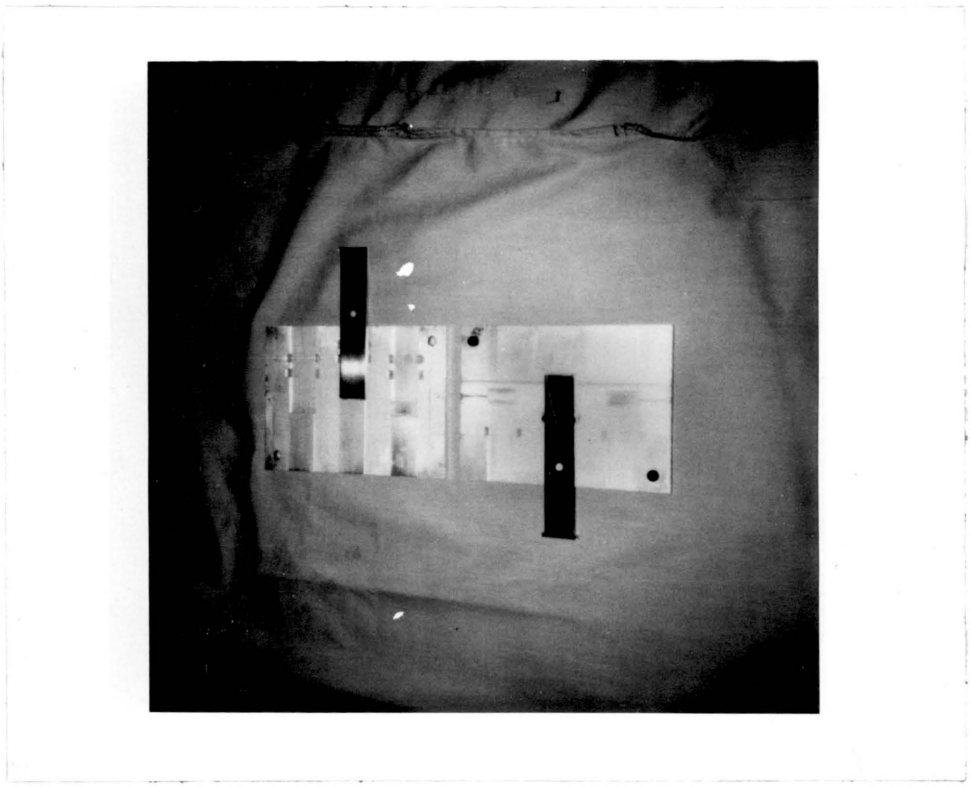

Figure 2-3 Open gluing jig showing placement of mating Ti 6-4 adherends

Uniformly sized sample discs of adhesives A2, B2, C2, D2, E2, polystyrene homopolymer, and polyisoprene homopolymer were punched from compression molded films, placed on surface treated titanium coupons, and left in an oven at 150°C for 10 minutes. The polystyrene homopolymer resided a total of 40 minutes at 150°C. The experiment was repeated at 200°C for new sample discs of the adhesives. The spreading patterns of the samples were recorded by photomicrography using the Polaroid Land Instrument Camera Model ED-10 on a Bausch and Lomb optical microscope. All samples were photographed at a magnification of 7X.

Investigation of Residual Stresses in Adhesives by Differential Scanning Calorimetry (DSC)

Effects of different temperature-pressure cycles on the strength of butt joints made from polystyrene and pyrex glass were reported by Vera, Baer, and Fort (47). They discovered the existence of a critical pressure at which permanent thermal stresses in the polystyrene adhesive were minimzed; hence, stronger adhesive joints resulted under that pressing condition. The implications of residual stresses induced by compression molding of styrene-containing adhesive films led to a differential scanning calorimetric study of two distinct pressing techniques for adhesive films. Frozen stresses in the styrene phase of the adhesive should be released in the vicinity of the styrene T_g (48). A high styrene content adhesive, E1, was therefore selected as the sample most likely to pronounce residual stresses due to pressing conditions. Three cases were analyzed by DSC:

1) Neat E1 powder as received from the Phillips Petroleum Co.,

2) Compression molded E1 film prepared as described previously, cooled under the applied pressure,

3) Compression molded E1 film prepared as follows: Neat copolymer was heated in the press at 150°C under 20,000 pounds pressure. After 10 minutes the applied pressure was released, and the sample was then allowed to remain at temperature for 3 minutes. Cooling to 65°C was performed without pressure on the film.

DSC thermograms were collected on the Perkin-Elmer DSC-2 over the temperature range 310-420K. The heating rate was 10K/min. The cooling rate was 40K/min. After cooling, a second and third scan were conducted on the same three samples. Two samples of each case were tested in this way to ensure reproducibility.

Mechanical Property Testing

Dumbell-shaped samples of the adhesives A1, B1, C1, D1, and E1 were stamped from their compression molded films for stress-strain experiments. Sample dimensions were 4.6 mm x 22.4 mm with sample thickness ranging from 0.5 to 1.0 mm. A smaller dumbell-shaped coupon (2.7 mm x 9.6 mm) was sometimes used. Stress-strain curves were obtained at room temperature using an Instron Model 1122 with a crosshead speed and temperature identical to that for joint failure tests (1 cm/min). The tensile moduli were evaluated from the initial slope of the stress-strain curve and were calculated for the different sample dimensions according to the formula:

$$E\ (\text{dynes/cm}^2) = \frac{ch}{cl} \times \frac{9.81 \times 10^{-3}\ (\ell)(cs)}{(xhs)(w)(t)}\ 10^7$$

where ch = chart height for slope in grams

cl = chart length for slope in mm

ℓ = sample length

cs = chart speed mm/min

w = sample width

t = sample thickness

xhs = crosshead speed mm/min

Rheology

Dynamic mechanical moduli and dynamic viscosities of SIS adhesives A3, B2, C1, D3 and E1 at temperatures ranging from 160 to 225°C were measured with the Rheometrics Mechanical Spectrometer (RMS) Model 605. Circular samples of 25 mm diameter were cut from compression molded adhesive films, and measurements were made in the parallel plate testing mode with a gap width of 0.5 mm for all samples. Strain amplitude was set at 10%. The test frequency was fixed at 1 Hz. Sample discs were maintained at the various test temperatures prior to measurement for times ranging from 3 to 30 minutes depending upon the visible evidence of melting and the magnitude of normal forces accompanying gap setting. A preliminary test of strain amplitude and time dependences of the dynamic viscosity and moduli of samples A2 and E1 confirmed the stability of the measurements over the range of residence times and the absence of sample degradation.

Scanning Electron Microscopy (SEM)

Areas selected for SEM studies were cut from the fractured adhesive layers, mounted with silver paint, and coated with a 40% paladium-60% gold alloy by vacuum evaporation. Surfaces of the titanium adherends before and after fracture were also examined and did not require coating. The scanning electron microscope used was an American Metals Research (AMR) 900 J-3. All samples were positioned for normal incidence of the electron beam.

CHAPTER 3

RESULTS AND DISCUSSION

Characterization of the SIS copolymer adhesives was performed in the six areas which comprise the designated dominant variables affecting the adhesive joint performance of these materials. This chapter is structured to present 1) the results of the adhesive characterization, 2) an assessment of the relative importance, rank, and relationship of the dominant variables studied, and 3) the emergence of other factors not originally considered among the dominant variables which proved to exert an overriding influence on the material properties of the adhesives and consequently, on adhesive performance.

Adherend Nature and Topography

The phosphate-fluoride surface treatment of titanum alloy coupons provided the means to achieve a uniform substrate nature and topography. Smith and Kaelble report that the titanium surface after phosphate-fluoride treatment is very rough (7). Figure 3-1 is a scanning electron photomicrograph of a freshly cleaned Ti 6-4 adherend. Surface rugosity is clearly evident. The photomicrograph actually represents the titanium dioxide layer on the adherend surface. Various workers (7) have disagreed on the oxide film thickness and structure (amorphous or crystalline rutile, anatase, or hydrated oxides). Alexander (7) found that bath temperatures and rinse times of the surface treatment determined the type of film

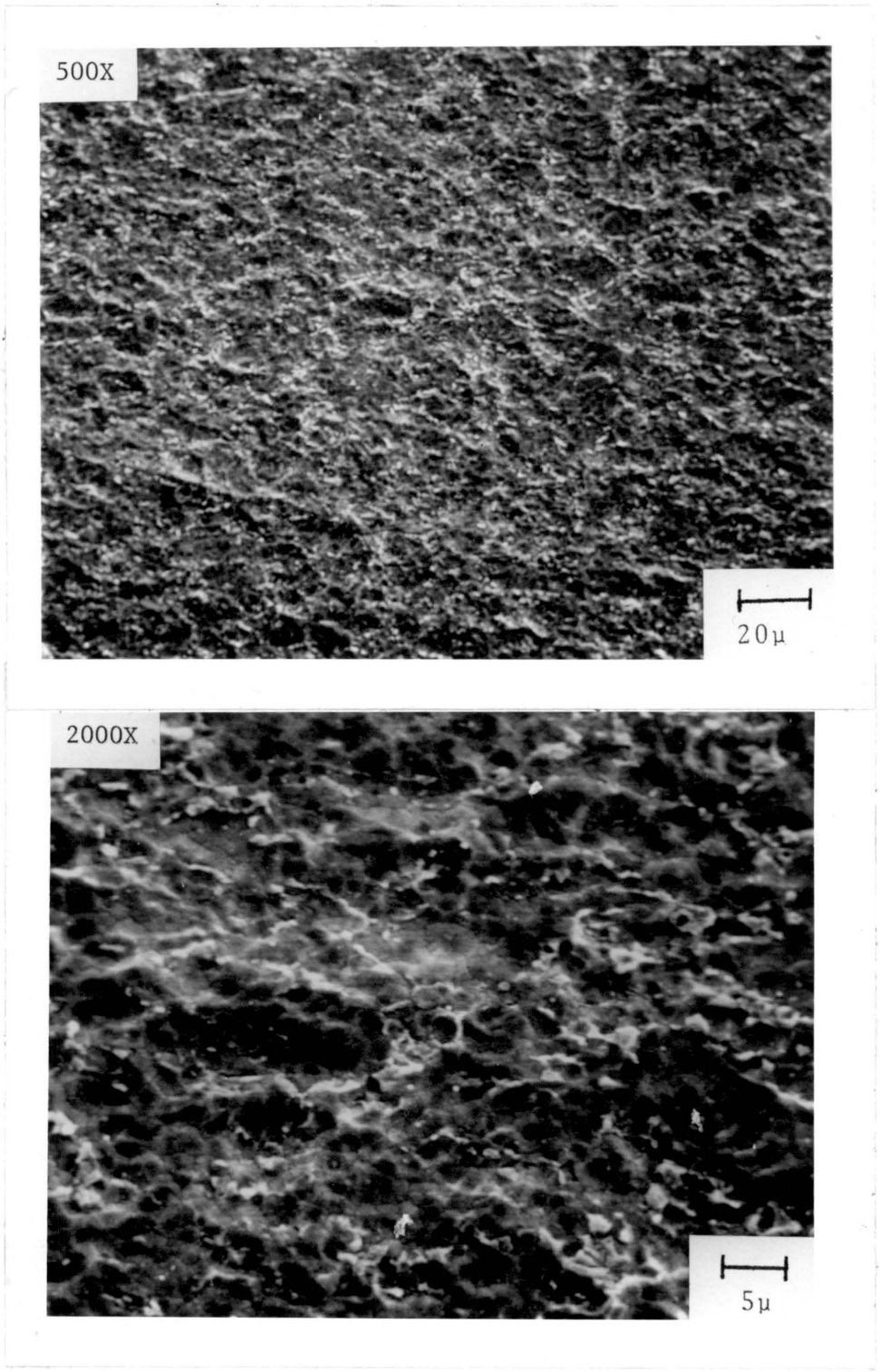

Figure 3-1 Scanning electron photomicrographs of a phosphate-fluoride treated Ti 6-4 adherend

formed and the bonding characteristics. Hence, strict adherence to the selected phosphate-fluoride treatment formulation was assumed to ensure a reproducible film layer.

Adhesive and Adherend Contamination

Using XPS analysis, Chen, et al. (42) reported phosphorous, fluorine, potassium and chlorine residues on Ti 6-4 after phosphate-fluoride surface treatment. Because the atomic percentages of these residues were 3% or less and contaminant adsorption on the cleaned alloy surfaces was minimized by the substrate storage conditions, SEM alone was deemed adequate confirmation of substrate uniformity and cleanliness.

As reported in Chapter 2, contamination of the adhesive films from compression molding was studied using XPS. Films pressed between aluminum sheets gave clean XPS spectra showing only traces of Si and an oxygen atom percent of 13.

Wetting

The primary step in adhesive joining of materials is good surface coverage of the substrate by the adhesive. Figure 3-2 shows the spreading patterns generated by adhesives A2 (20% styrene content) and E2 (60% styrene content) on surface treated Ti 6-4 after 10 minutes at 150°C and also at 200°C. The results for these two compositions are presented to emphasize the contrasts of spreading behavior for the extremes of styrene content in the adhesive series. Sample A2, like homopolyisoprene (Figure 3-3), demonstrated obvious wetting of the

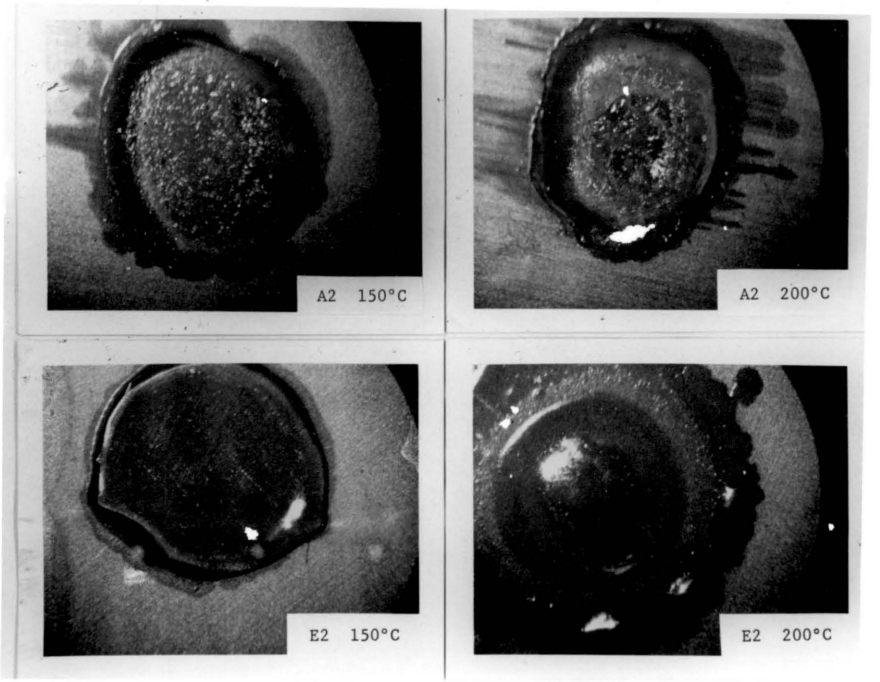

Figure 3-2 Spreading patterns for adhesives A2 and E2 on phosphate-fluoride treated Ti 6-4

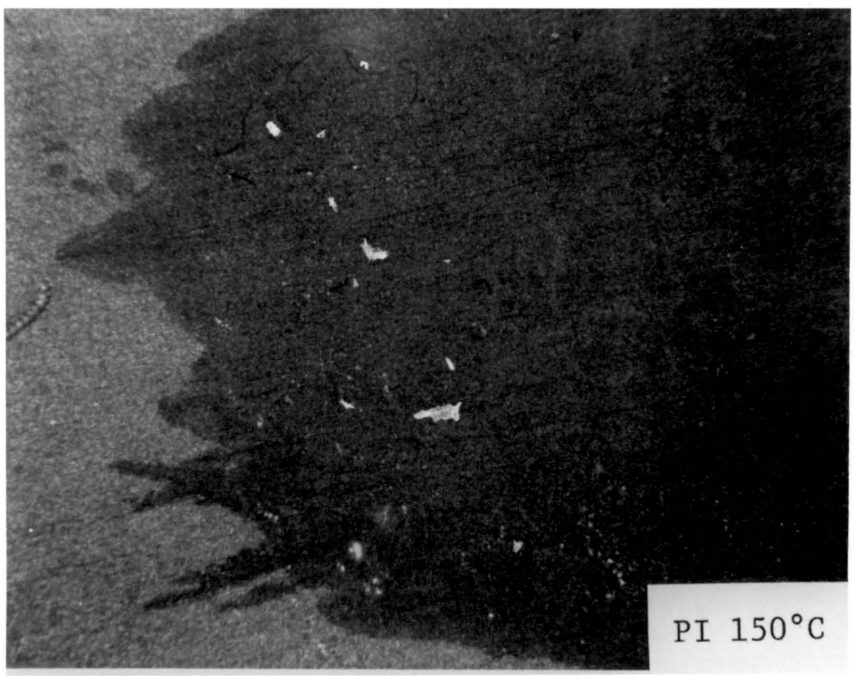

Figure 3-3 Spreading pattern for homopolyisoprene on phosphate-fluoride treated Ti 6-4

titanium substrate as the spreading film appears to have conformed to and was channeled by mill lines on the metal surface. This pattern of spreading behavior was observed for all adhesives with a styrene content of 40% or less. Sample E2 also showed spreading on Ti 6-4 at 150°C; however, the spreading pattern did not appear to be influenced by substrate topography. The absence of wetting accompanying spreading of the adhesive film was implied. Figure 3-4 shows the lack of spreading by homopolystyrene on Ti 6-4 after 40 minutes at 150°C. Although good contact without spreading was observed for polystyrene on the substrate at elevated temperature, removal of the sample from the oven resulted in delamination of the styrene sample from the metal as the polymer cooled below its T_g.

At 200°C both low and high styrene content adhesives maintained their respective spreading patterns, although sample E2 spread over a larger radius. This behavior can be attributed to a decreased viscosity of the samples at 200°C vs. 150°C. Also, the molecular weight of sample E2 is 3-1/2 times smaller than that of A2 and should display a more dramatic difference in viscosity-controlled spreading rates than would A2 whose viscosity even at 200°C is still relatively high. The enhanced spreading pattern of E2 at 200°C might also result from reduced viscosity due to increased phase mixing in the adhesive. Widmaier and Meyer (29) optically confirmed a loss of ordered structure in an SIS film of similar composition (38% isoprene, but lower molecular weight than E2) as sample temperature was raised. However, the change from an originally anisotropic film to an

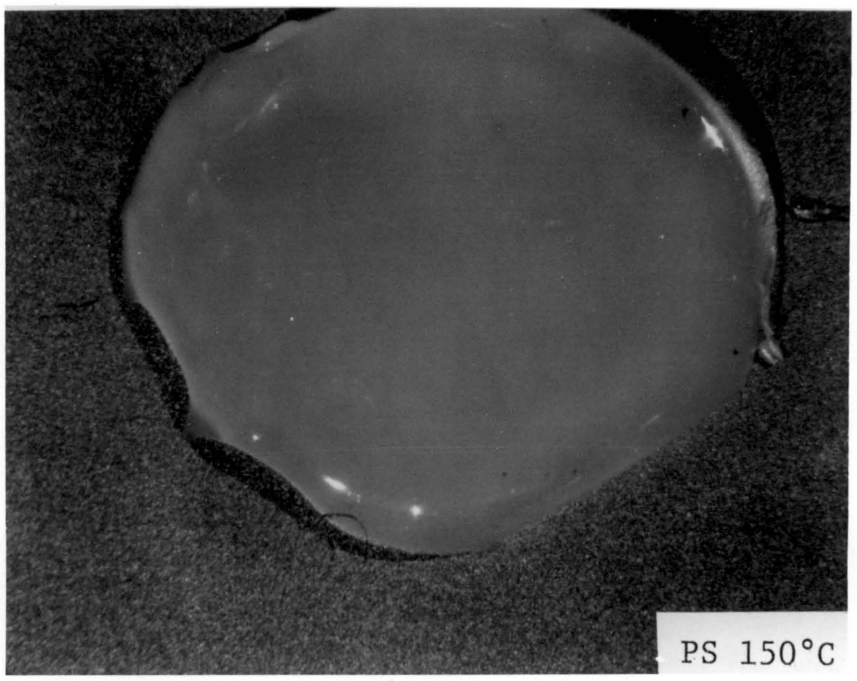

Figure 3-4 Homopolystyrene on phosphate-fluoride treated Ti 6-4 after 40 minutes at 150°C

isotropic condition required at least 1.5 hours at 200°C or longer for lower temperatures. Such a time constraint suggests that the 10 minute limit at the testing temperatures of the spreading experiment was insufficient to produce a homogeneous melt. The spreading pattern of sample E2 at 200°C should still reflect that of a two-phase system; consequently, it can be concluded that spreading is not significantly inhibited under these conditions for any of the SIS adhesives. Because spreading does not appear to be viscosity limited for these materials at joint formation temperatures, surface coverage of the titanium substrate is assured, and the contribution of the wetting variable to adhesion of these systems can be considered relatively equal.

Residual Stresses in SIS Adhesive Films

Differential scanning calorimetry thermograms for (I) E1 copolymer powder, (II) compression molded E1 film cooled under film formation pressure, and (III) compression molded E1 film cooled without applied pressure are shown in Figure 3-5. The glass transition temperature for styrene, defined as the midpoint of a characteristic baseline change of the DSC trace, falls at 98°C for these samples. In addition to the baseline change at the T_g, curves I and II exhibit another baseline change (endothermic) centered at 70°C. This event could result from residual solvent from synthesis of the copolymer, lower molecular weight molecules, or from the release of stresses "frozen" in the styrene phase of the adhesive during thermal and mechanical processing. Solvent contamination of the adhesive is

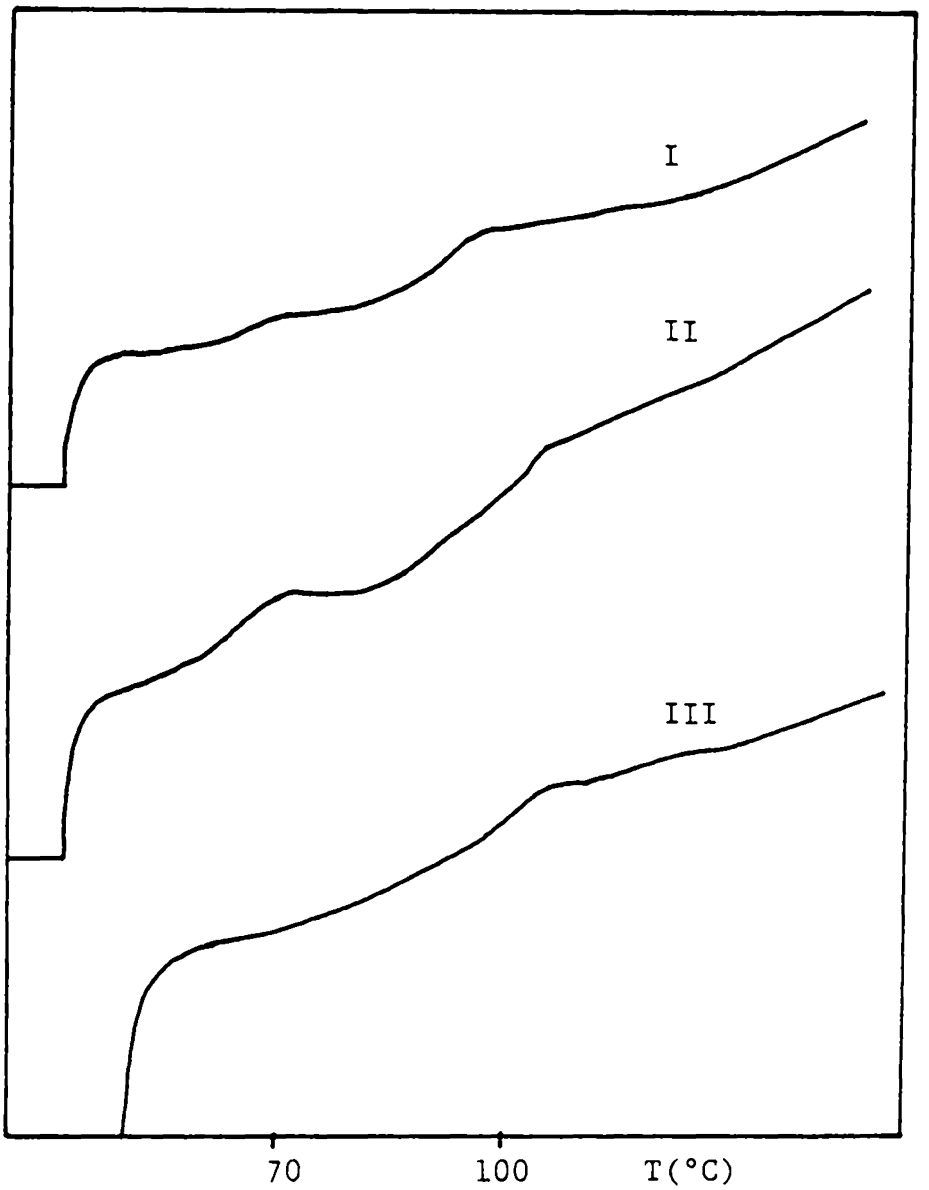

FIGURE 3-5: FIRST RUN DSC CURVES FOR SAMPLE E1 (I) POWDER, (II) COMPRESSION MOLDED FILM COOLED UNDER PRESSURE, (III) COMPRESSION MOLDED FILM COOLED WITHOUT PRESSURE

not a reasonable explanation for the pre-T_g thermal event. The process of compression molding (sample II) would have removed the solvent prior to DSC analysis of the adhesive film. Low molecular weight molecules which could demonstrate a lower T_g than higher molecular weight blocks of polystyrene and thus account for the event at 70°C would be expected in all 3 curves. Furthermore, a second DSC scan of these materials should show the low molecular weight residues. But Figure 3-6 reveals that the second DSC scans of these samples do not reproduce the first traces containing the low temperature event. For new samples of E1 powder and films the thermal event occurs reproducibly in the first DSC scan for samples I and II but disappears in the second scan. It can be concluded that the baseline change observed in the copolymer powder and accentuated in the compression molded film cooled under pressure results from stress-releasing phenomena within the polystyrene domains of this adhesive. The compression molded film cooled without applied pressure never produced a larger low temperature event than was present in the E1 powder sample. This compression molding technique apparently contributes no additional residual stress to the resulting films and is thus a superior film preparation method for adhesive applications.

Joint Formation Temperatures and Failure Behaviors

Widmaier and Meyer (33) reported a joint preparation temperature dependence of shear strength for lap joints made from SIS materials containing 30%, 48%, and 65% isoprene by block length. Optimum tensile shear strengths were observed for each composition at

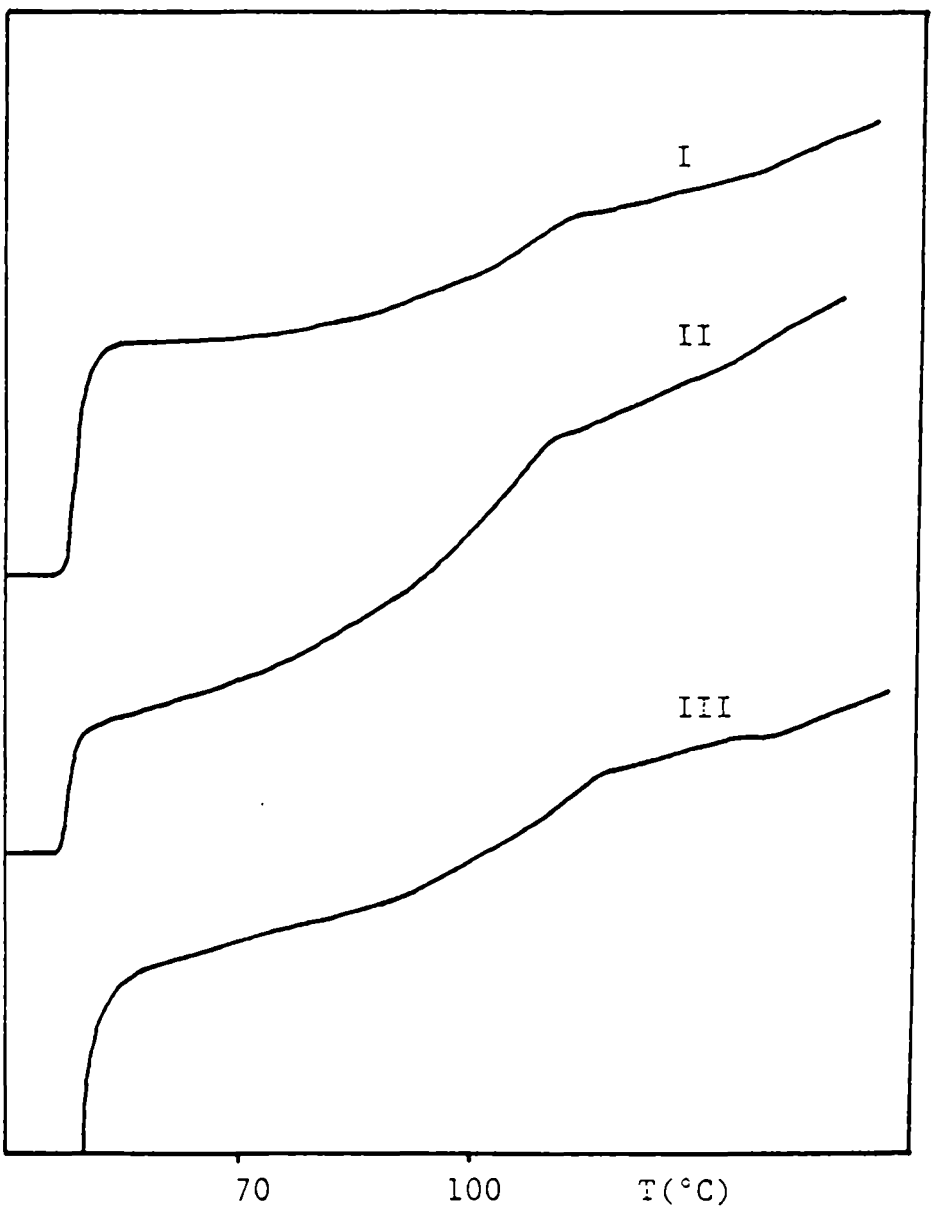

Figure 3-6. Second run DSC curves of sample E1 (I) powder, (II) compression molded film cooled under pressure, (III) compression molded film cooled without pressure, after quenching from first run curves of figure 3-5

different temperatures which these workers attributed to conditions of equal block viscosities. Their calculations to that effect could not be confirmed by this investigator, nor was a joint formation temperature dependent joint strength observed in this study for the SIS containing 50% styrene by weight. Table 3-1 summarizes the temperature/joint strength data. The reported joint strengths are averages of 5 lap specimens. Within the standard deviation of the measurements the joint strengths corresponding to the different preparation temperatures are equivalent. A temperature dependency may not have been observed because of a significantly higher fracture testing speed used in the present study. Also, these joints were allowed a 10 minute temperature exposure while Widmaier and Meyer's work employed a 2 hour activation period. It is known that a 2 hour residence time around 150°C is sufficient to alter the two-phase morphology of all but very high molecular weight SIS materials. Temperature dependence of SIS joint strengths might be linked to a homogeneous state of the adhesive melt in joint preparation.

Fracture of the lap joints prepared for the study of temperature dependence of joint strength revealed dichotomous adhesive behavior. These joints were prepared from compression molded adhesive films. Figure 3-7 presents distinct failure curves produced by adhesive D1. Some lap specimens fractured with quick, brittle debonding of the adhesive layer from one titanium adherend. Others demonstrated ductile drawing of the adhesive layer and elongation of the original bond area by 200-400% prior to ultimate joint failure. The two

Table 3-1

Effect of Joint Preparation Temperature on the Average Joint Strength of Adhesive D1

Joint Preparation Temperature (°C)	Average Joint Strength ± σ (N/cm^2)
130	390 ± 40
160	410 ± 80
180	420 ± 40

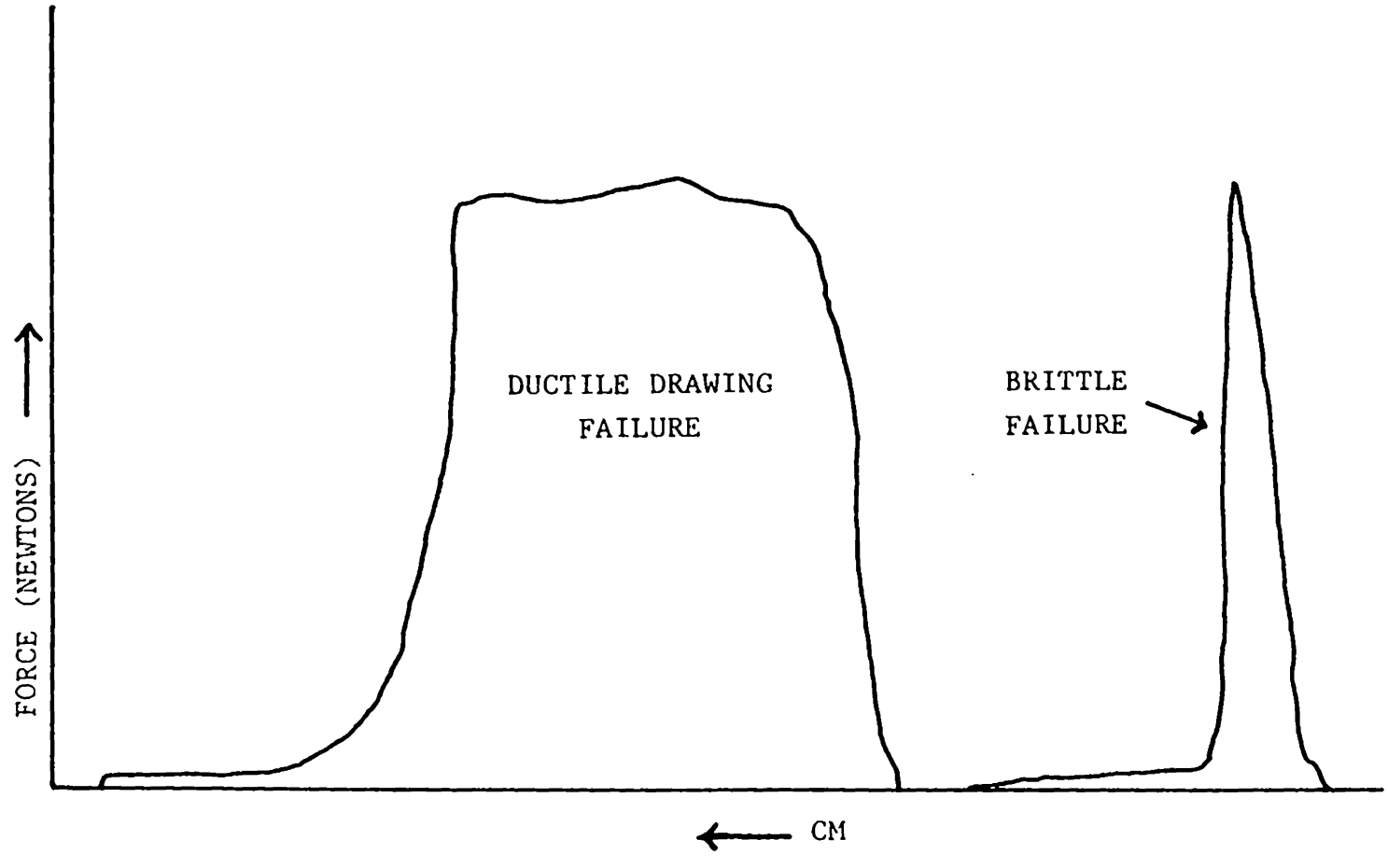

Figure 3-7. Typical failure curves for adhesive D1

failure curves were observed in all sets of D1 adhesive joints regardless of the temperature of joint formation; however, the ductile failure occurred more often in the set of joints prepared at 130°C. Results of the mechanical property testing and rheology of the SIS materials reported in the following sections lend support to the belief that the distinct failure curves produced by the D1 system are related to the presence of microphase domains in the adhesive. In the compression molded films of SIS copolymers these domains are multi-directional. In adhesive D1 the microphase structure, lamellar, would not be uniformly oriented throughout the film, and adhesive layers cut from the film might reflect the mechanical properties of a predominant orientation. At lower joint formation temperatures the copolymer molecules have less mobility than at higher temperatures where there was averaging of the effect of domain directionality.

Mechanical Properties

Film anisotropy was evident in the results of initial tensile modulus measurements for various SIS adhesives. Table 3-2 presents data for repeat determinations of initial tensile moduli for the range of styrene contents of the adhesive series. For some compositions both small and large sizes of dumbell-shaped samples were tested. Agreement of repeat determinations is good for the low styrene content adhesives. Beginning with sample C1 at 40% styrene content, the volume fraction of styrene (0.37) dictates a cylindrical structure of the microphase domains and the first appearance of a styrene connective morphology. The irreproducibility of the tensile modulus

Table 3-2

Reproducibility of Initial Tensile Modulus Measurements for SIS Adhesive Series

Sample	Weight Percent Styrene	Initial Tensile Modulus ($dynes/cm^2$) Large Dumbell Sample	Small Dumbell Sample
A1	20	1.5×10^8 1.5×10^8	
B1	30	6.6×10^8 7.0×10^8	
C1	40	1.2×10^9 7.2×10^9	9.4×10^8 9.5×10^8
D1	50	5.9×10^9	1.9×10^9 2.1×10^9
E1	60	7.1×10^9	3.3×10^9 6.7×10^9

value for large-size specimens of this material suggests distinct moduli for different arrangements of styrene cylinders. Nielsen (12) discusses the various moduli defined for anisotropic materials. Precision of modulus measurements improves for smaller sample sizes of C1 film. Yet the magnitude of the modulus for small samples still differs from that for large samples of the same film. Adhesives D1 and E1 also demonstrate an influence of sample size on the tensile modulus despite the fact that the modulus calculations include sample dimension factors. The planar random anisotropy (biaxial orientation) of a connected styrene phase in these higher styrene content adhesives could account for the irreproducibility which is emphasized for larger sample areas and improved for smaller sample sections.

For either sample size the trend of increasing modulus with increasing styrene content can be generally accepted, and the effect of limited domain orientation in these films does not cause the tensile modulus of a given adhesive composition to defy a characteristic range associated with that styrene content.

Rheology

Figure 3-8 presents a plot of the dynamic viscosity at 1 Hz vs. temperature for the series of SIS compositions. The shaded points are repeat measurements for a particular composition and temperature. Obviously, the anticipated trend of decreasing viscosity with temperature is not consistently observed, and reproducibility between different samples of a given adhesive is poor. Rather than smooth, negatively sloping curves for each adhesive which might have provided

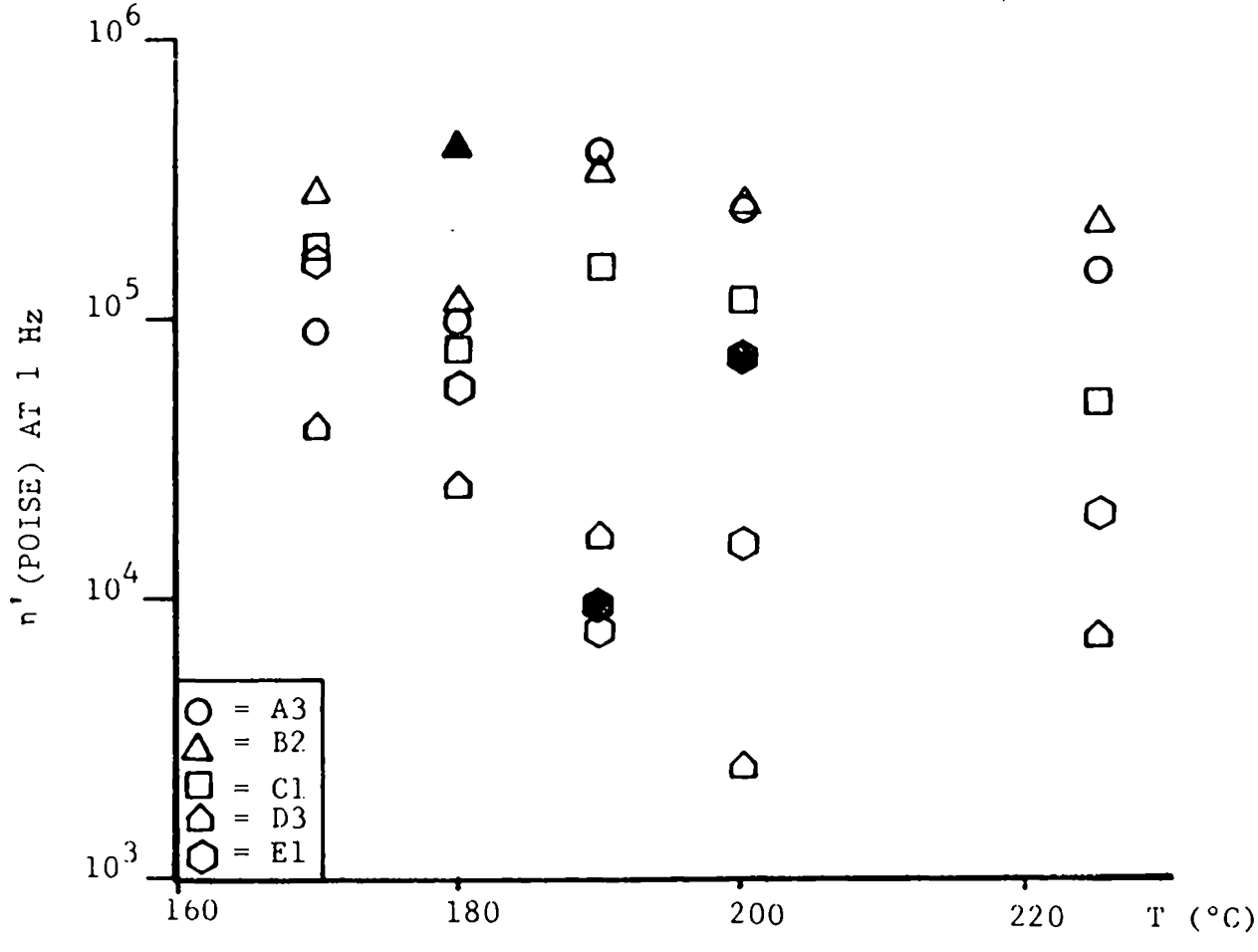

FIGURE 3-8. Dynamic viscosity at 1 Hz vs. temperature for the series of SIS adhesives. Shaded points represent repeat measurements.

isoviscous data for the different compositions, points for a given adhesive are widely scattered and afford several interpretations:

1) the scatter of the data points is characterized by a low and high region possibly corresponding to different morphological states for samples of one composition,

2) the scatter pattern might be interpretted as a temperature independence of the melt dynamic viscosity (see data points for sample B2),

3) the magnitudes of the dynamic viscosities are essentially molecular weight controlled, although at lower temperatures inversions occur.

From the rheological literature on SIS and SBS materials it was discovered that the test frequency chosen for this study is near a threshold value for the reported flow transition that occurs at low frequencies with increased temperature for these triblock copolymers (27, 29, 30, 51). A growing consensus ascribes the transition to dissolution or disintegration of styrene domains at higher temperatures. It would seem that the low and high regions of dynamic viscosity measurements produced by the adhesives may reflect the pre- and post-transition morphologies characteristic of the SIS rheology. On the other hand, the molecular weights of the adhesives studied here are double those used for rheological work to date on SIS. The theoretical critical equilibrium temperature at which phase miscibility is achieved may not be attained for these materials before degradation occurs. Specific viscosity measurements conducted before and after the Rheometrics testing were nearly identical, confirming little, if any, sample degradation at the highest temperatures employed for this study. However, the only reported flow transition

for an SIS system is between 215-225°C for a fairly low molecular weight material (45,000) (29). The molecular weights of these adhesives range from 65,000 to 157,000. Given these molecular weights and the relatively short residence times at testing temperatures (3-30 minutes) the likelihood that a post-transition morphology (homogeneous melt) could be produced is questionable. The anisotropic character of these SIS films persisting in the melt is a more probable explanation of the rheological scatter.

Kamal and Utracki's (49) review section of rheology of block polymers states that the low shear rate values of viscosity and the primary normal stress difference coefficient are very sensitive to sample history. Steady shear cone and plate experiments conducted on an SBS have shown that shear stress-time traces vary in shape with shear rate, and that a constant shear stress value is never reached for any shear rate less than $1.8s^{-1}$ (50). Consequently, calculation of viscosity becomes arbitrary. Significant differences were noted in the magnitude of the viscosity depending upon the time period between measurements and these differences were greatest at lower shear rates. The time dependence of normal stresses was extremely great as well. Because different time and normal stress conditions were required in the present study to achieve the same gap setting for thick films (A3 and B2) as for thin films, large variation in normal stress with time could have contributed to a pre-testing, irreproducible shear history of the samples.

Residual stresses were also reported in the SBS after cessation

of steady shear (50). The magnitude of residual stress depended on the time of previous shear deformation. Despite typical disparity of steady state and dynamic viscosity values for block copolymers, the processes of domain deformation of the original sample structure are consistent for both modes at low frequency testing, and one could expect these similar shear and thermal history effects in dynamic measurements. Chung and Lin (51) present data for the dynamic viscosity of a SBS copolymer vs. temperature over a wider temperature range than the present study. The thermal history (pretest treatment) and gap conditions for the samples are not reported but significant scatter of the data is demonstrated at most frequencies, particularly near the flow transition temperature.

In summary, the selected frequency (1 Hz) for the rheological work on the SIS adhesives inadvertently emphasized the effects of inconsistent stress and thermal histories of each sample, compounded by the uncertain and possibly irreproducible morphological state of the copolymer melt. Although these complicating factors might have been minimized by modified procedures at higher testing frequencies, limited sample supply precluded another rheological study at more favorable experimental conditions. Moreover, the higher frequency data would not be as appropriate for simulation of adhesion processes.

Orientation of Adhesive Films: Effects on Joint Failure

The marked influence of an uncontrolled directionality, or more generally, anisotropy, of the compression molded SIS films on

mechanical and rheological properties of the adhesives, particularly at higher styrene contents, led to the preparation of oriented adhesive films by extrusion techniques. Oriented films were intended to provide a uniform domain allignment in the extrusion direction so that the morphological variable could be contained. Table 3-3 summarizes joint strength and fracture energy data for lap shear joints prepared with the orientation direction of the adhesive layer either parallel or perpendicular to the fracture axis of the joint. Due to limited material the values for sample E2 are an average of two lap specimens for each orientation while for the remaining compositions, the values represent an average of six joints. Joint strengths increase with increasing styrene content reflecting the trend of higher adhesive tensile modulus; but for a given composition the effect of adhesive orientation on the average joint strength is negligible. The important comparison is that of the fracture energies of the different orientations for sample E2. The high fracture energy for the parallel orientation corresponded exclusively to the ductile drawing failure curve noted earlier. The perpendicular orientation produced only the brittle failure curve and low fracture energies. For adhesives D3, C2, and the Kraton (SBS) the correlation between orientation and failure types was not so clear. Both ductile and brittle failure behaviors were observed in both orientations for these materials.

At lower styrene fractions, especially for a spherical domain morphology, significant orientation effects would not be expected.

Table 3-3

Orientation Study

SAMPLE	% STYRENE	FRACTURE AXIS ORIENTATION	AVERAGE JOINT STRENGTH (N/cm^2)	AVERAGE FRACTURE ENERGY (J)
E2	30	∥	430 ± 70	3.9 ± 0.8
		⊥	380 ± 40	1.3 ± 0.1
D3	50	∥	290 ± 40	3.0 ± 1.0
		⊥	320 ± 60	2.6 ± 0.6
C2	40	∥	210 ± 40	2.6 ± 0.7
		⊥	180 ± 10	2.1 ± 0.9
Kraton	30	∥	50 ± 10	3.0 ± 1.0
		⊥	50 ± 10	2.5 ± 0.9

Distinct orientations with respect to the joint fracture axis would not appear until styrene connected domains such as cylinders or lamellae were present. Adhesives D3 and C2 possess one of these morphologies based on their volume fractions of styrene. The fact that a clear correlation between fracture energy and adhesive orientation could not be made for these samples may reflect

1) effects of a different extrusion temperature than that of E2,

2) incomplete orientation due to a low extrusion rate and lack of take-up tension (Although the highest rotor speed available on the extruder was employed, the rate of extrusion for these highly viscous materials was too slow to apply take-up tension without tearing the film.),

3) the implication that the orientation effects are only segregatable for adhesive compositions approaching a styrene continuous morphology. This conclusion should be verified through elimination of variables 1) and 2). That is, for a constant extrusion temperature, quantitation of film orientation is needed to confirm the quality of domain allignment for the different adhesive morphologies.

Another important contribution to the orientation study would be data on elastic moduli for the separate (and optimized) orientations of each adhesive composition. The variation in moduli with orientation should be compared among the higher styrene content materials to assess the relative importance of this property to the joint behavior.

Scanning Electron Microscopy (SEM)

Features of the fracture surfaces of both adhesive and adherend are easily probed using SEM, but full characterization of an adhesive

failure mechanism cannot be attempted by examining, in this case, a quarter section of each of a few selected samples in a group of failed specimens. Recurring features do appear for some samples albeit without predictable regularity. For others the same feature becomes conspicuous by its absence and thus, lends an implied specificity to its interpretation. For the SIS adhesives the fracture surfaces observed by SEM were restricted to the low (20% or Kraton) and high (60%) extremes of styrene content. In these two categories considerable differences in the recurring failure characteristics were found. For low styrene content materials failure was localized in the form of "fibers" pulling out of the adhesive layer appearing to cause crazes. Figures 3-9, 3-10, and 3-11 present typical views of this phenomenon. Figure 3-12 shows the raised adhesive surface as a fiber begins to emerge and open the crevice. In Figure 3-13 these fibers appear in a surface craze possibly as they are under the adhesive surface before extension.

Because the Kraton is an oriented adhesive sample, the direction of fiber formation is of interest; in Figures 3-10 and 3-14 the fiber direction should be noted. In both micrographs the fracture axis (direction of applied force) is vertical. In Figure 3-10 the film is oriented horizontally. Failure occurs predominatly in the unoriented direction. In Figure 3-14 the film is oriented vertically, and failure occurs primarily in the weaker, horizontal direction.

Scanning electron photomicrographs of fracture surfaces of SIS or SBS have not been found in the literature. Beecher (52) has published

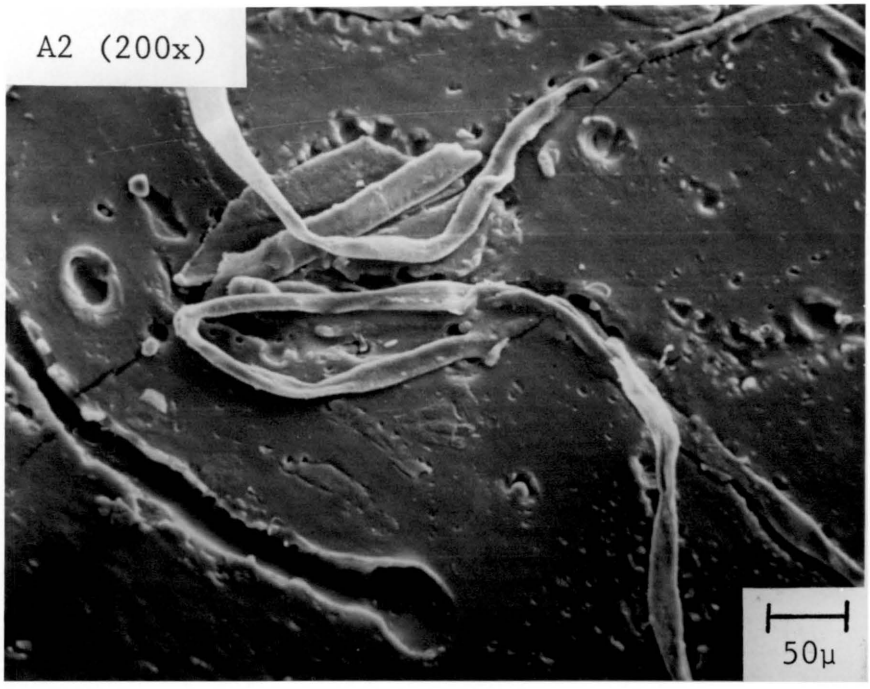

Figure 3-9 Photomicrograph of fractured A2 showing fibers on surface

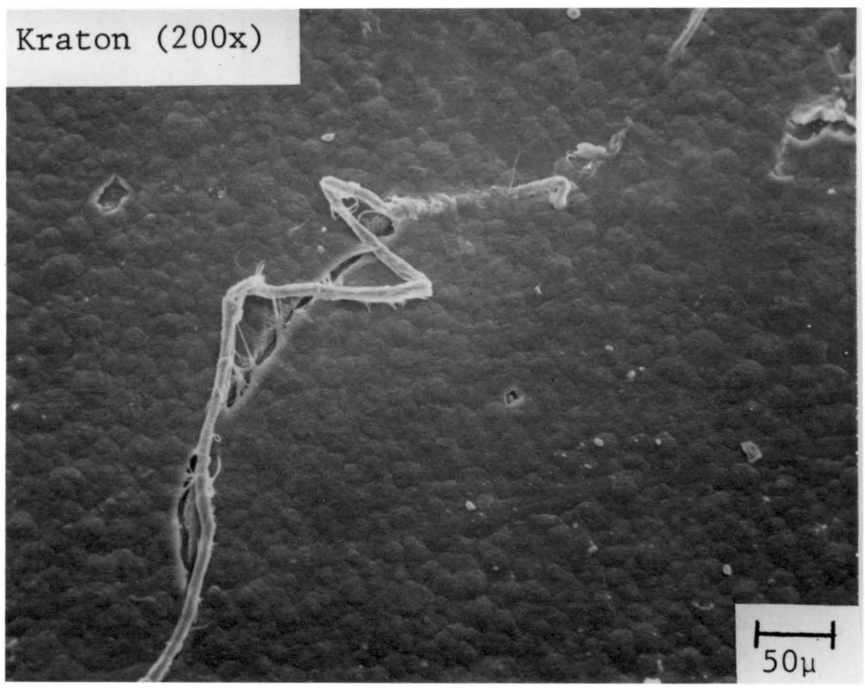

Figure 3-10 Photomicrograph of fractured Kraton (oriented vertically) showing fiber formation

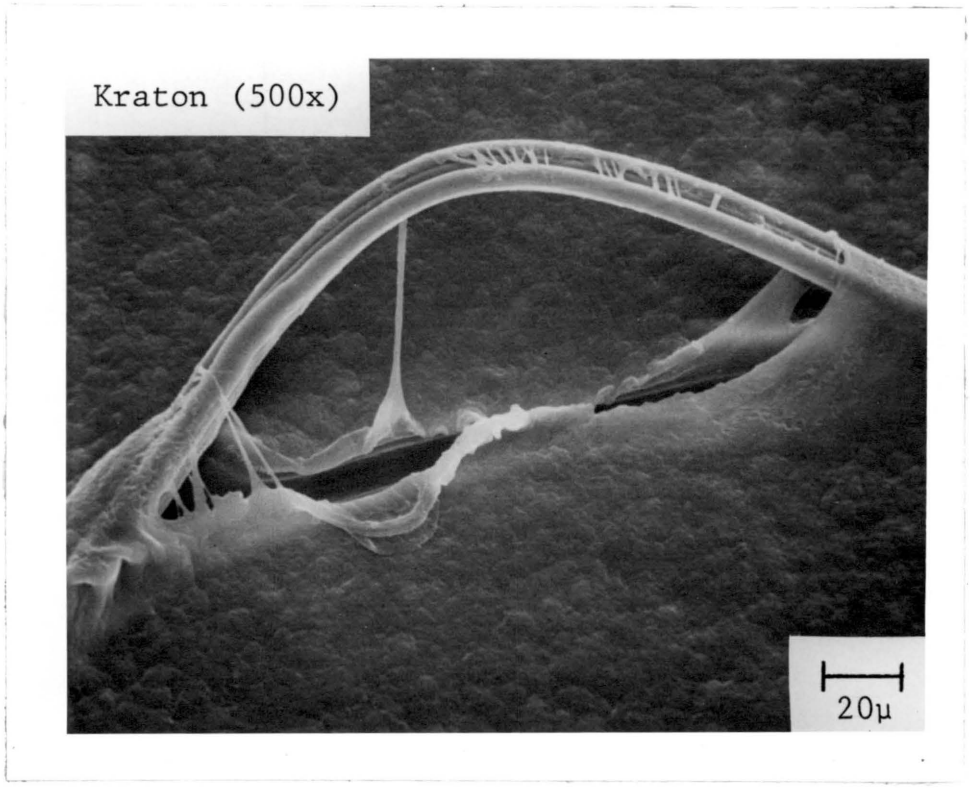

Figure 3-11 Photomicrograph of fractured Kraton (oriented vertically) showing deformation of adhesive surface as fiber emerges

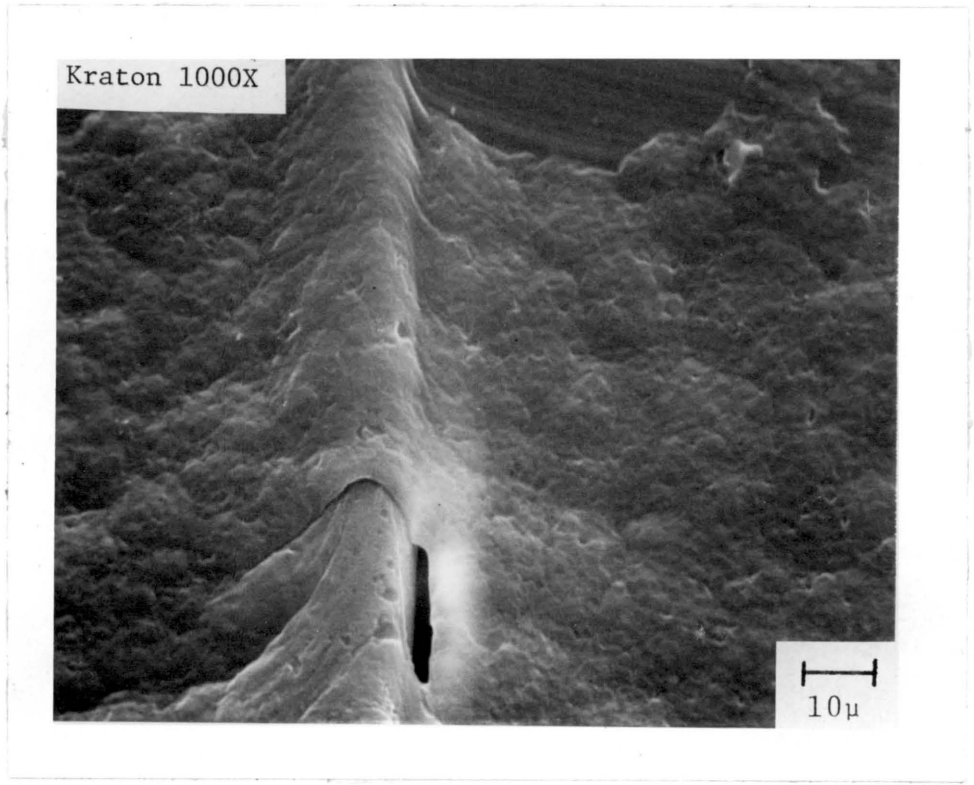

Figure 3-12 Photomicrograph of Kraton showing raised adhesive surface and crack initiation around underlying fiber

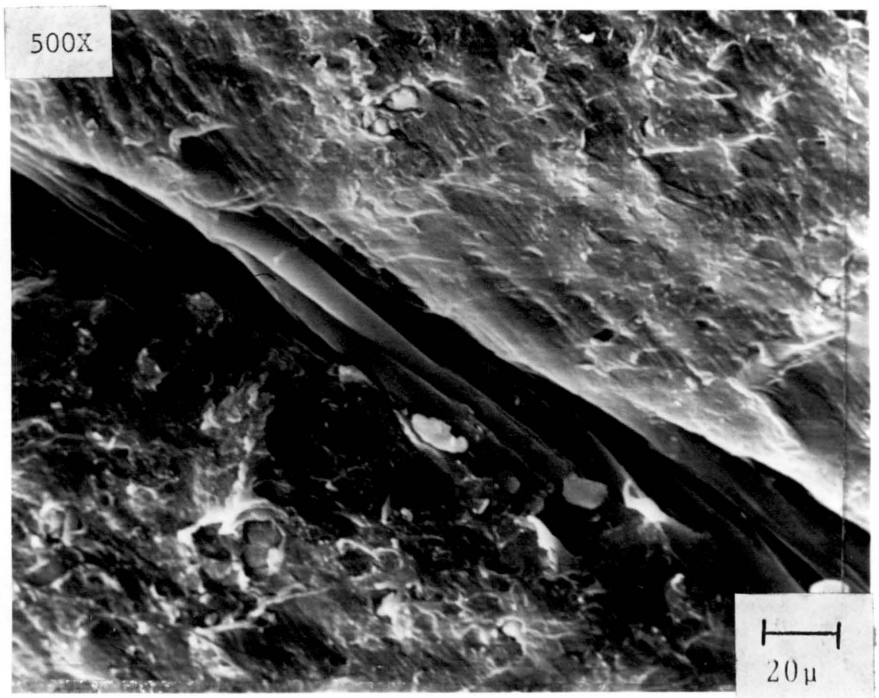

Figure 3-13 Photomicrograph of fibers lying in open crevice

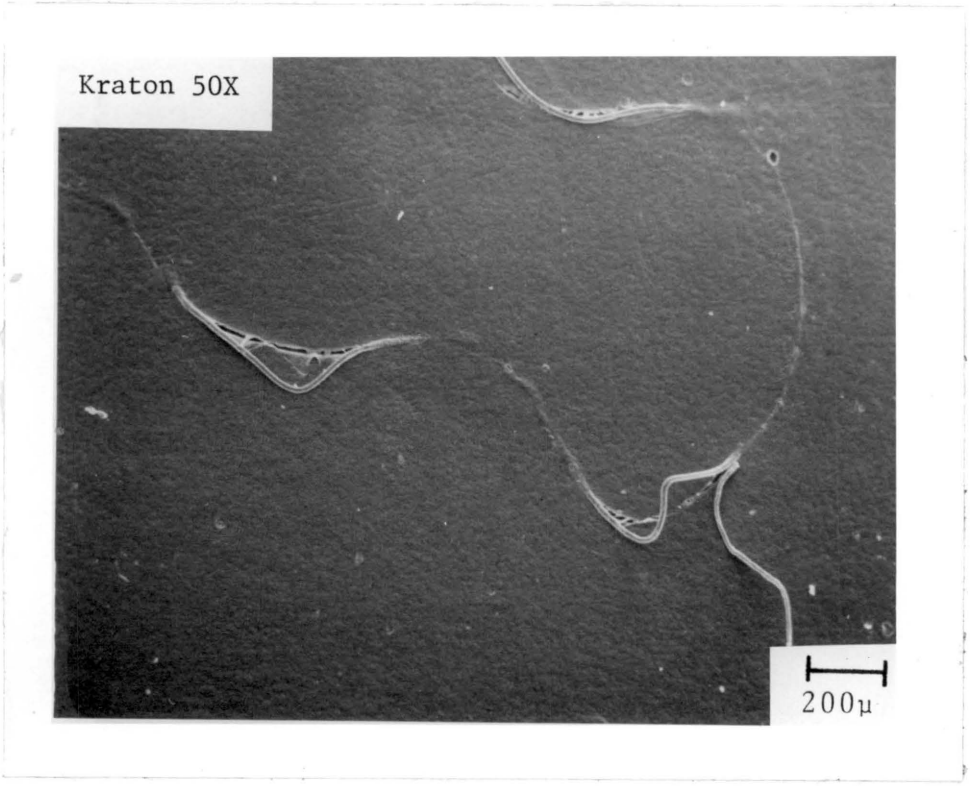

Figure 3-14 Photomicrograph of fractured Kraton (oriented vertically)

transmission electron micrographs of SBS films deformed in tension. He states that failure of the materials is always preceded by considerable deformation of the styrene domains "with the system tending toward fully extended polystyrene molecules. Rupture always occurs in the polystyrene phase." Haward and Brough (23) report the presence of fibers in flexurally fractured high molecular weight polystyrenes. Their micrographs are similar to Figures 3-15 and 3-16 although the fiber sizes in their samples are much smaller. These workers postulated that the fibers formed when the material was temporarily heated during adiabatic deformation preceding crack growth. This mechanism does not appear suited for the copolymer adhesives; however, a relationship between fiber formation and the polystyrene component of these materials can be inferred.

Failure features in the high styrene adhesive composition are shown in Figures 3-17 through 3-20. Failure is not as localized. Larger areas of the adhesive surface demonstrate plastic deformation and flow (Figures 3-17 and 3-20). The fine structure seen in the flow regions of Figure 3-20 reflects the orientation direction (horizontal) for this adhesive film. Again, for all micrographs the fracture axis is vertical. The high styrene content adhesive obviously demonstrates a greater ability to dissipate the fracture energy than do the low styrene content materials. In this respect the SEM work confirms the widely held concept that an adhesive which can dissipate the energy supplied to a joint during fracture processes forms stronger adhesive bonds through this mechanism.

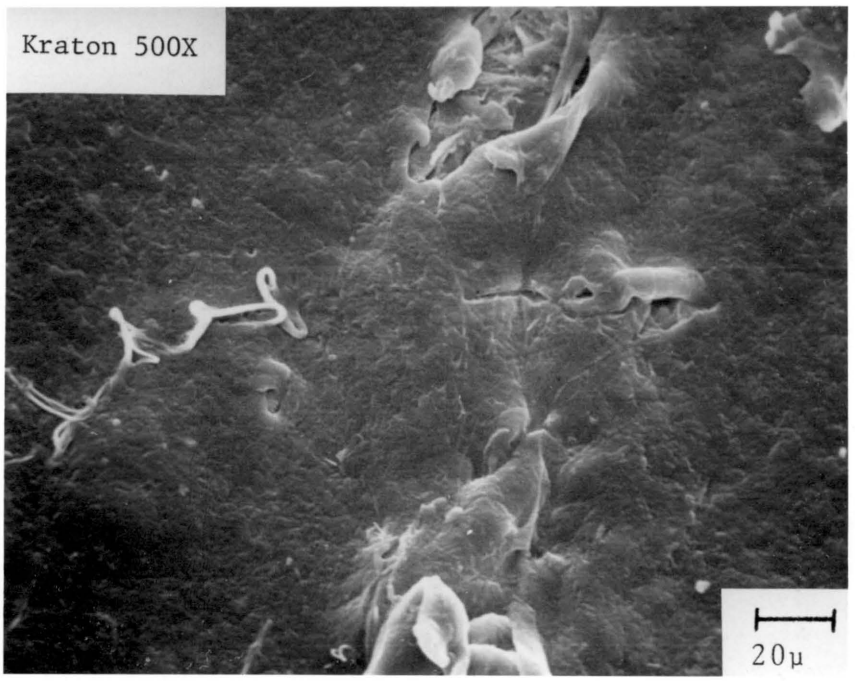

Figure 3-15 Photomicrograph of fractured Kraton showing smaller fibers at left

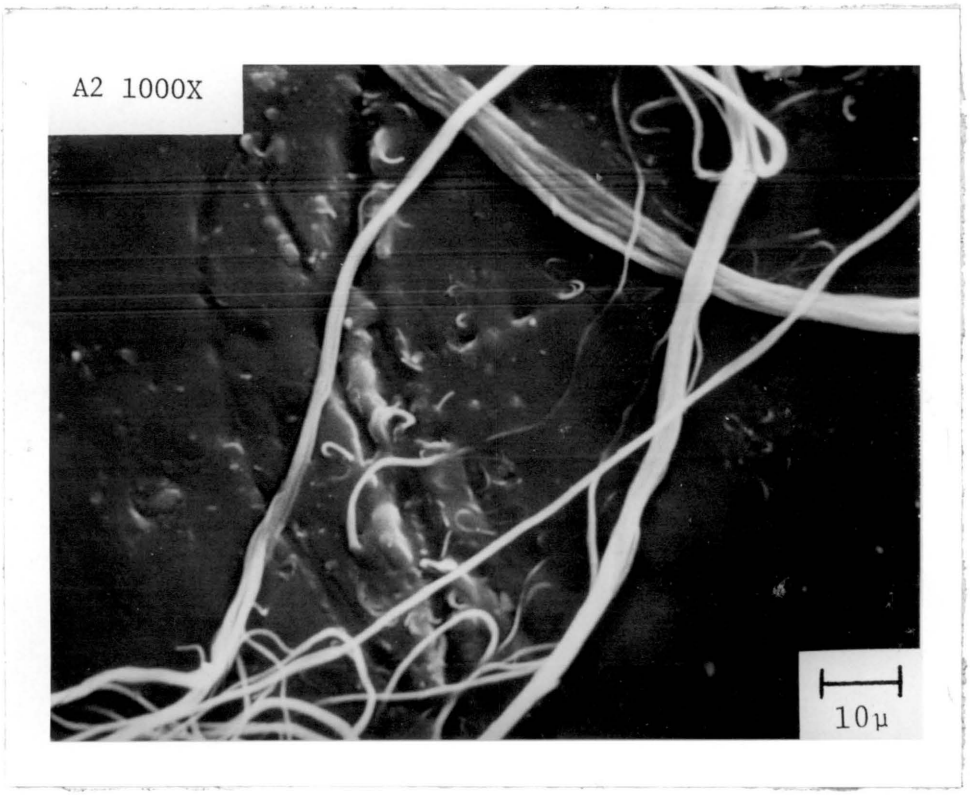

Figure 3-16 Photomicrograph of fractured A2

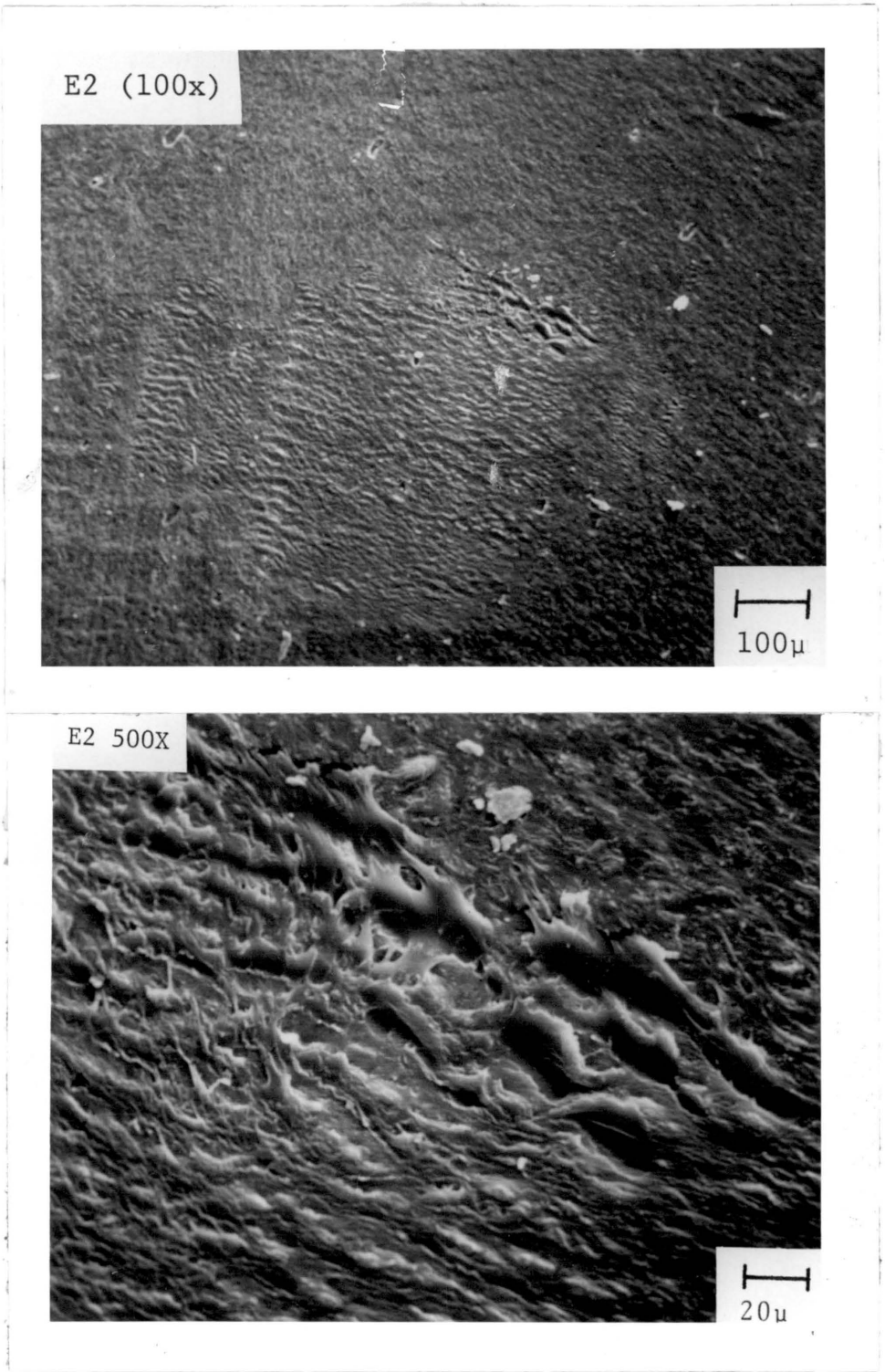

Figure 3-17 Photomicrographs of fractured E2. Bottom: enlarged area from center top

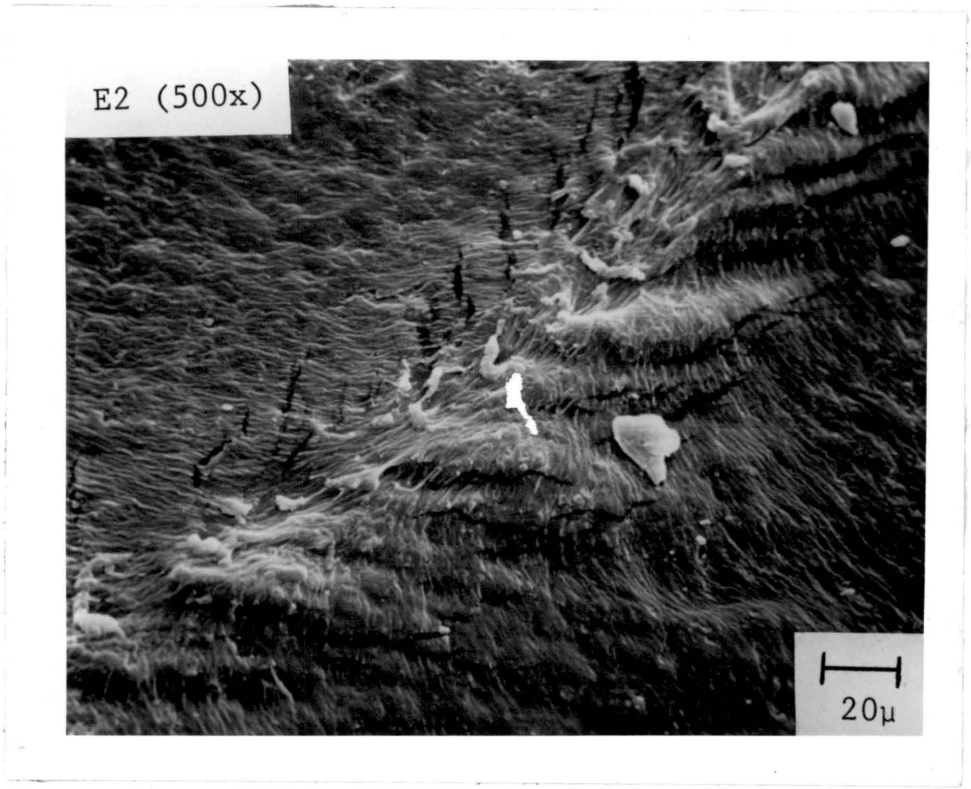

Figure 3-18 Photomicrograph of fractured E2 showing sectional motion

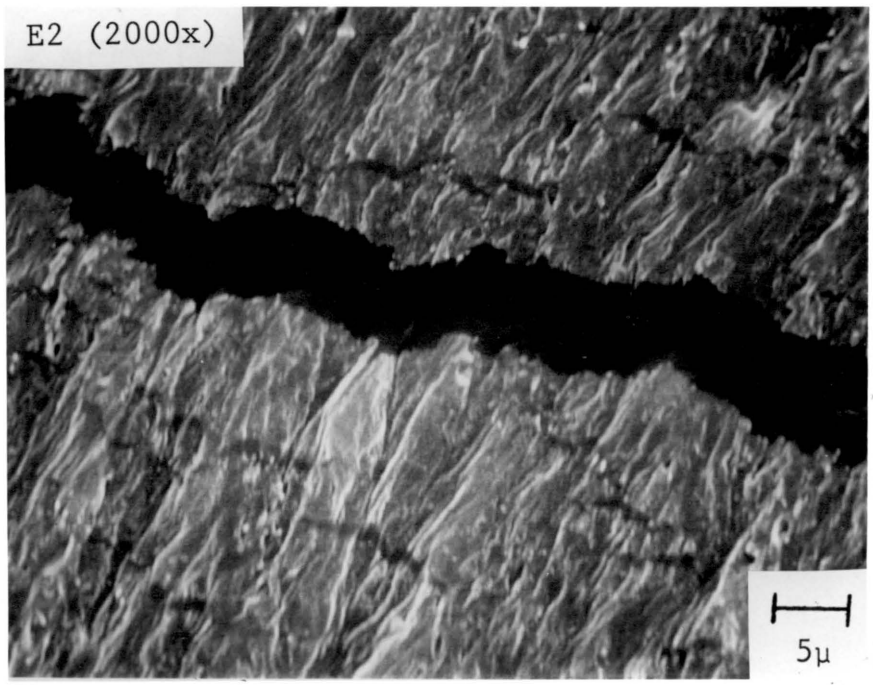

Figure 3-19 Photomicrograph of fractured E2 surface divided by clean, brittle break

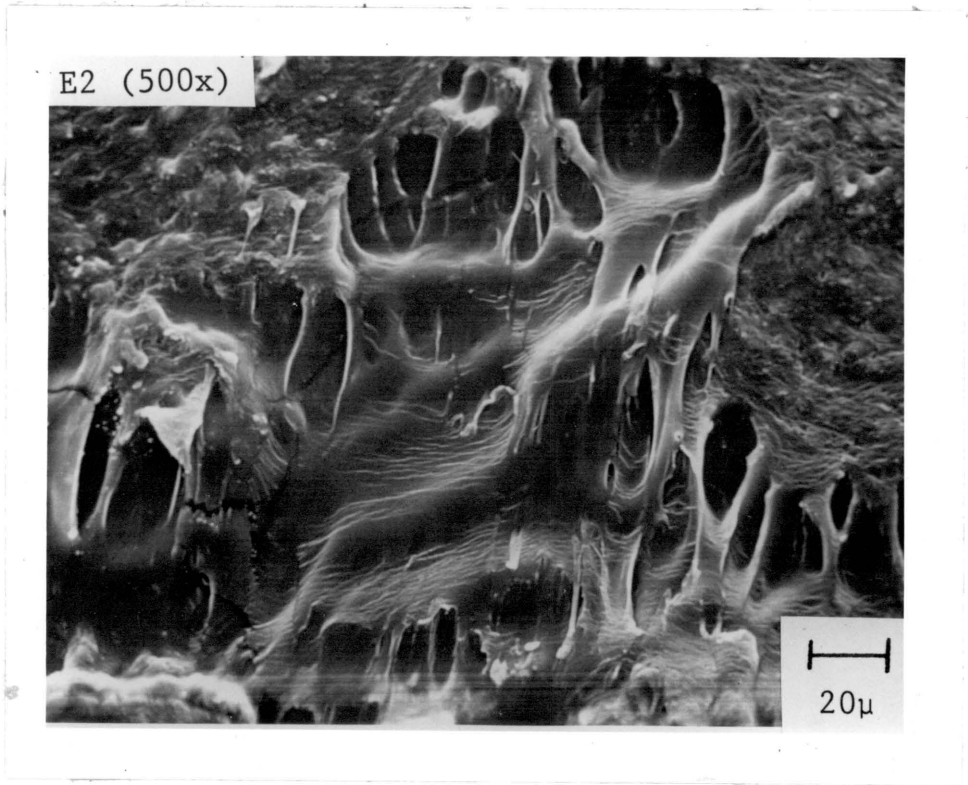

Figure 3-20 Photomicrograph of fractured E2 (oriented horizontally) showing plastic flow deformation

Figures 3-21 and 3-22 are included to point out another fiber formation process observed in the high styrene SIS and attributed by Parsons, et al. (24) to cohesive failure in peel of high molecular weight polystyrene. The micrographs were taken of an adhesive section that had stretched and stress-whitened in joint failure. The progression described by Parsons and clearly seen in the SIS samples is one of cavitation and coalescence resulting in fiber formation. Both of these phenomena result in an increase in the stress-bearing region, the latter being the larger contributor. Indeed, the joints demonstrating these effects had higher adhesive strengths and fracture energies than samples of the same composition without stress-whitening.

For low and high styrene content adhesives joint failure appeared to be interfacial on visual inspection. With SEM the fractured adherend surfaces showed interfacial and cohesive failure and the presence of long fibers on surfaces mated with the low styrene content adhesives (Figure 3-23 and 3-24).

Summary: The Dominant Variables in Retrospect

The results of characterization of the SIS copolymer adhesives in terms of the dominant variables point to the fact that certain of these variables can be successfully eliminated as in the case of residual stresses in adhesive films and their composite joints. The wetting factor did not contain major distinctions between adhesive samples and was not considered a primary contributor to differences in adhesion qualities; however, one recognizes the necessity of

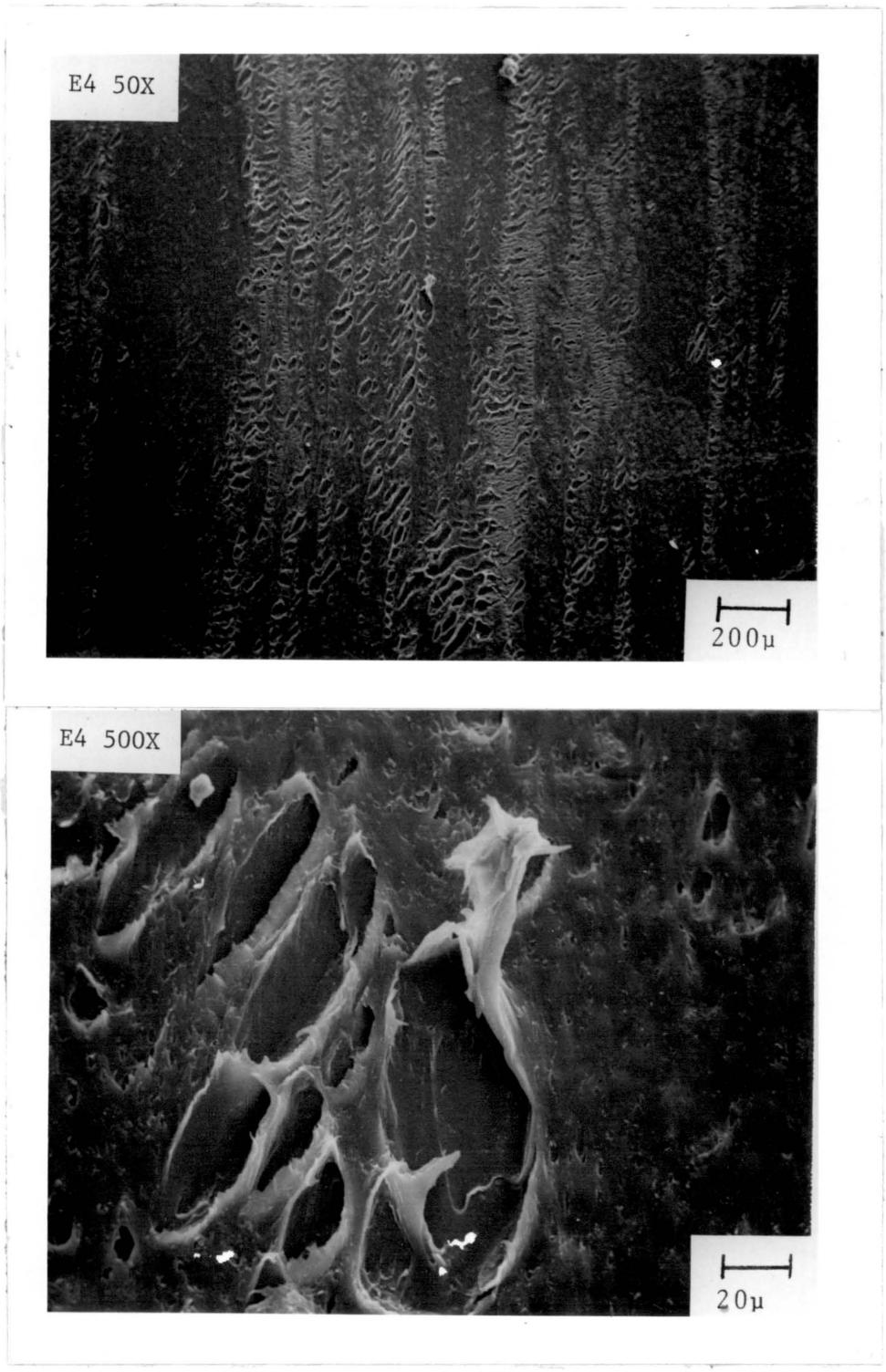

Figure 3-21 Photomicrographs of fractured E4 showing cavitation-coalescence sequence. Bottom: enlarged area from center top

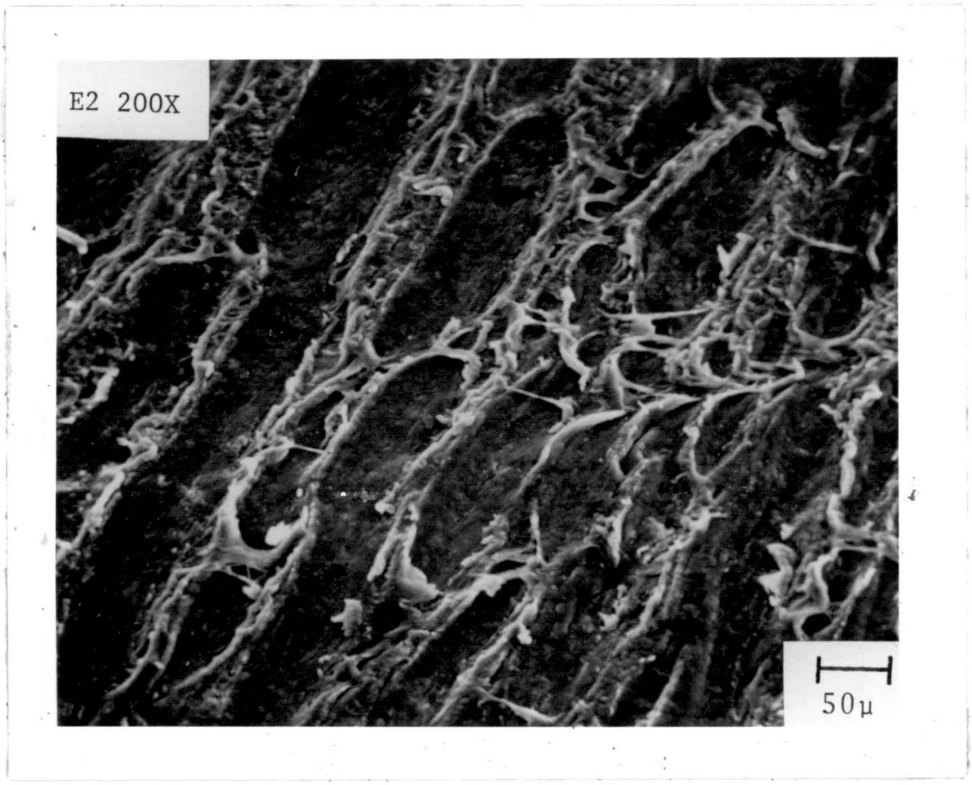

Figure 3-22 Photomicrograph of fractured E2 showing cavitation - coalescence fiber formation

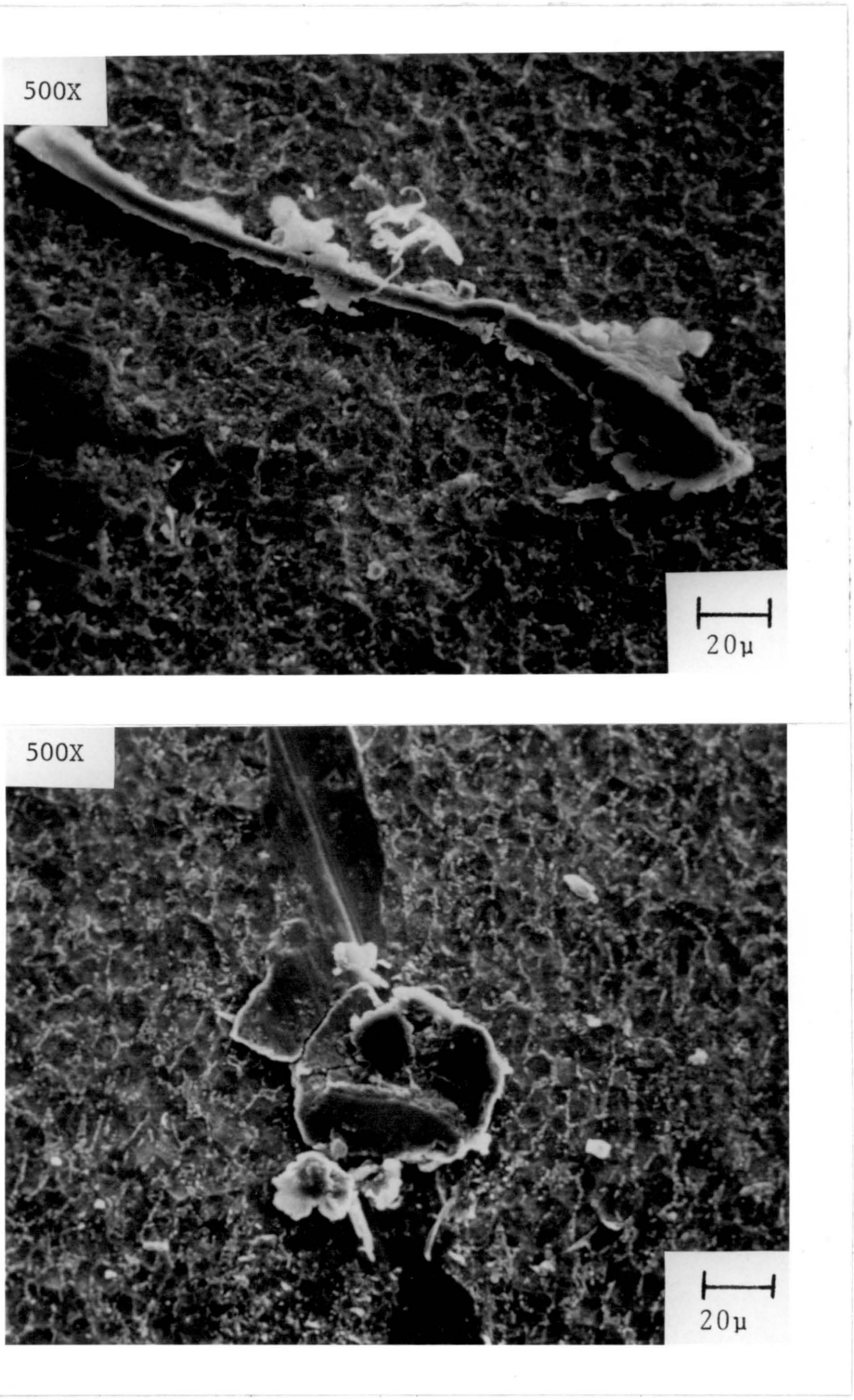

Figure 3-23 Photomicrographs of fractured Ti 6-4 adherend from E2 system showing cohesive and interfacial failure

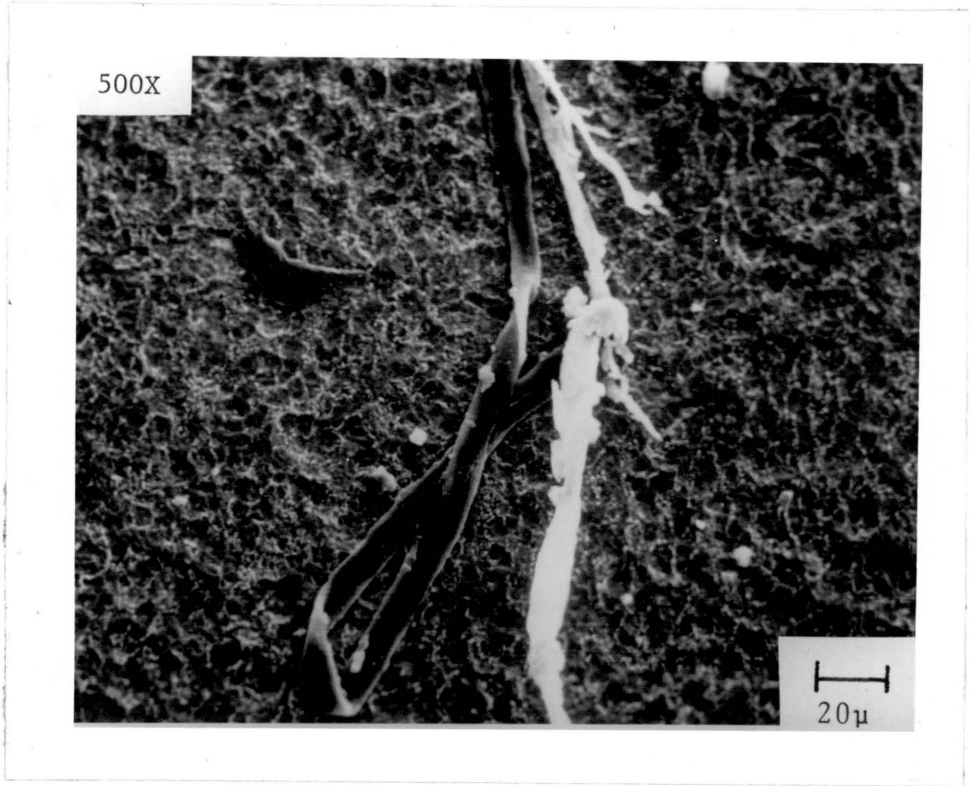

Figure 3-24 Photomicrograph of fractured Ti 6-4 adherend from A2 system showing fibers on surface

producing good joints through wetting in order to assess all other factors influencing joint behavior. Joint performance seemed to most closely parallel trends in the mechanical and morphological properties of the adhesive series, and so these factors should be ranked at the top of the list of dominant variables. Also the important contribution of viscoelastic processes in the mechanisms of failure of these adhesive joints couples with the role of substrate topography and its capacity to enhance energy dissipation.

CHAPTER 4

CONCLUSIONS

This study as an overview of variables and mechanisms affecting the adhesion of SIS copolymers has been successful despite inability to completely fulfill the original project objective. First, the high molecular weights of the adhesive series were prohibitive for accurate rheological work but raised the importance of producing a defined morphological state (one-phase or two-phase) for similar rheological and adhesion study. Second, some dominant variables were successfully eliminated from all the adhesive systems such as residual stresses in the styrene phase of the materials. A preferred pressing technique for hot-melt adhesive applications of thermoplastic elastomers was defined. Third, joint behavior most closely parallelled the mechanical property and morphological trends of the adhesive series. The joint fracture energy, in particular, was affected by styrene domain connectivity and orientation. Finally, SEM presented distinct failure characteristics for fracture surfaces of low and high styrene content SIS adhesives. The mechanisms of cohesive failure of these materials through various degrees of energy dissipation processes confirmed that highly dissipative adhesives form stronger bonds. From another view the significant difference in moduli of low and high styrene content adhesives may have dictated different stress distributions in the lap joints of these two materials activating different failure modes.

CHAPTER 5

RECOMMENDATIONS FOR FUTHER STUDY

From the assessment of the variables studied for SIS adhesive performance the emergence of morphological and orientation factors command further attention. If adhesion studies continue for the two-phase condition of these materials, clearly a characterization of degrees of orientation (possibly by dichroism) for cylindrical and lamellar morphologies should be obtained and correlated with joint failure data, especially with fracture energies. Folkes and Keller (53) describe extrusion methods for preparation of "single-crystal" (uniformly oriented rod and lamellae microphases) SBS materials which may be of interest. Mechanical property data for these orientations would be helpful in explaining orientation effects on joint performance.

The objective to control dominant variables should be amended for a defined morphological state of the SIS materials. That is, more rheological data are needed, preferrably on lower molecular weight samples to determine a reproducible copolymer melt for the different adhesive compositions. The objective might also be extended to fracture conditions by employing a failure test that 1) produces one mode of failure (peel vs. a peel and shear combination in the lap joint) and 2) controls failure initiation through some uniform built-in flaw. The cantilever beam test affords these benefits and provides a more equitable stress distribution for different adhesive systems. Also, the fracture mechanics analysis of this test

specimen is very simple (54). Otherwise, SEM identification of adhesive surfaces failed exclusively in peel, shear, cleavage, etc. might assist in evaluating fracture mechanisms in mixed mode failure testing.

Finally, for continued adhesion work on SIS systems it should be noted that the literature to date is focused on styrene continuous compositions, lower molecular weights, and probably isotropic or homogeneous material. Any of the above recommendations should be considered for styrene continuous systems as well as for the isoprene continuous adhesives studied in this work. Particularly, the orientation study points to improved correlations with a styrene continuous adhesive.

References

1. A. J. Kinloch, J. Mat. Sci., 15, 2141 (1980).

2. S. Wu, in Polymer Blends, Vol. 1, ed. by D. R. Paul and S. Newman, Academic Press, N.Y., 243 (1978).

3. D. K. Ryder, Principles and Applications of Adhesives, predates the Journal of Educational Modules for Materials Science and Engineering, Materials Research Laboratory, The Pennsylvania State University, University Park, PA.

4. L. H. Sharpe and H. Schonhorn, Advances in Chemistry Series, 43, ed. by R. F. Gould, A. Chem. Soc., Washington, 189 (1964).

5. R. N. Wenzel, Ind. Eng. Chem., 28, 998 (1963).

6. D. M. Brewis and D. Briggs, Polymer, 22(1), 7 (1981).

7. T. Smith and D. H. Kaelble, in Treatise on Adhesion and Adhesives, Vol. 5, ed. by R. L. Patrick, Marcel Dekker, N.Y., (1981).

8. J. J. Bickerman, The Science of Adhesive Joints, Academic Press, N.Y., (1968).

9. H. Schonhorn and R. H. Hansen, J. Polym. Sci. B4, 203 (1966).

10. J.R.G. Evans and D. W. Packham, Int. J. Adhesion and Adhesives, 149, (January, 1981).

11. W. D. Bascom and R. L. Patrick, Adhesives Age, 17(10), 25 (1974).

12. L. E. Nielsen, Mechanical Properties of Polymers and Composites, Vol. 1, Marcel Dekker, N.Y., (1974).

13. G. Holden, E. T. Bishop, and N. R. Legge, J. Polym. Sci. C, 26, 37 (1969).

14. L. E. Nielsen, Polymer Rheology, Marcel Dekker, N.Y., (1977).

15. L. Greenwood, Aspects of Adhesion, Vol. 5, ed. by D. J. Alner, CRC Press, Cleveland, Ohio, 40 (1968).

16. A. N. Gent and G. R. Hamed, Rubber Chem. and Tech., 51, 354 (1977).

17. J. Shields, Adhesives Handbook, Butterworth and Co. Ltd., London, (1970).

18. G. P. Anderson, S. J. Bennett, and K. L. DeVries, Analysis and Testing of Adhesive Bonds, Academic Press, N.Y., (1977).

19. R. J. Morgan, J. Polym. Sci., Polym. Phys. Ed., 11, 1271 (1973).

20. A. N. Gent, Adhesives Age, 25(2), 27 (1982).

21. C. A. Dahlquist, in Adhesion: Fundamentals and Practice, MacLauren & Sons, Ltd., London, (1966).

22. R. J. Bird, J. Mann, G. Pogany and G. Rooney, Polymer, 7, 307 (1966).

23. R. N. Haward and I. Brough, Polymer, 10, 724 (1969).

24. W. F. Parsons, M. A. Faust, I. E. Brady, J. Polymer Sci., Polym. Phys. Ed., 16, 775 (1978).

25. D. H. Kaelble, Physical Chemistry of Adhesion, Wiley-Interscience, N.Y., (1971).

26. A. Noshay and J. E. McGrath, Block Copolymers: Overview and Critical Survey, Academic Press, N.Y., (1977).

27. C. I. Chung and J. C. Gale, J. Polym. Sci., Polym. Phys. Ed., 14, 1149 (1976).

28. M. Iskandar and S. Krause, J. Polym. Sci., Polym. Phys., Ed., 19, 1659 (1981).

29. J. M. Widmaier and G. C. Meyer, J. Polym. Sci., Polym. Phys. Ed., 18, 2217 (1980).

30. E. V. Gouinlock and R. S. Porter, Polym. Preprints, Am. Chem. Soc., Div. Polym. Chem., 18(1), 245 (1977).

31. G. C. Meyer and J. M. Widmaier, Macromolecules, 14, 823 (1981).

32. J. M. Widmaier and G. C. Meyer, Polymer, 19, 398 (1978).

33. J. M. Widmaier and G. C. Meyer, Polymer, 18, 587 (1977).

34. G. C. Meyer and J. M. Widmaier, Polym. Eng. Sci., 17(11), 803 (1977).

35. D. F. Leary and M. C. Williams, J. Polym. Sci., Part B, 8, 335 (1970).

36. A. Weitz and B. Wunderlich, J. Polym. Sci., Polym. Phys. Ed., 12, 2473 (1974).

37. M. Iskandar, Ph.D. Thesis, Rensselaer Polytechnic Institute, 1981.

38. G. Kraus and J. T. Gruver, J. Appl. Polym. Sci., 11, 2121 (1967).

39. G. Kraus, F. E. Naylor and K. W. Rollmann, J. Polym. Sci., Part A-2, 9, 1839 (1971).

40. K. R. Arnold and D. J. Meier, J. Appl. Polym. Sci., Polym. Phys. Ed., 14, 1149 (1976).

41. S. Futamura and E. A. Meinecke, Polym. Preprints, Am. Chem. Soc., Div. Polym. Chem., 18(1), 268 (1977).

42. W. Chen, D. W. Dwight, W. R. Kiang, and J. P. Wightman, presented at the 4th International Symposium on Contamination Control, Washington, D.C., Sept. 13, 1978.

43. S. Mostovoy and E. J. Ripling, J. Appl. Polym. Sci., 13, 1083 (1969).

44. E. Orowan, Fatigue and Fracture of Metals, MIT Press, Cambridge, 139 (1950).

45. G. Kraus, K. W. Rollmann, R. A. Gray, J. Adhesion, 10, 221 (1979).

46. F. Delale and F. Erdogan, Viscoelastic Analysis of Adhesively Bonded Joints, Lehigh University, 1980, private communcation.

47. R. Vera, E. Baer, and T. Fort, J. Adhesion, 6, 357 (1974).

48. B. Wunderlich, in Thermal Characterization of Polymeric Materials, ed. by E. A. Turi, Academic Press, N.Y., (1981).

49. L. A. Utracki and M. R. Kamal, Polym. Eng. Sci., 22(2), 96 (1982).

50. A. Ghijsels and J. Raadsen, Pure Appl. Chem., 52, 1359 (1980).

51. C. I. Chung and M. I. Lin, J. Polym. Sci., Polym. Phys. Ed., 16, 545 (1978).

52. J. F. Beecher, L. Marker, R. D. Bradford, and S. L. Aggarwal, Polym. Preprints, Am. Chem. Soc., Div. Polym. Chem., 8(2), 1532 (1967).

53. M. J. Folkes and A. Keller, J. Polym. Sci., Polym. Phys., Ed., 14, 883 (1976).

54. R. Y. Ting and R. L. Cottington, Adhesives Age, June 1981, 35.

55. D. W. Dwight and W. M. Riggs, J. Colloid and Interface Sci., 47(3), 650 (1974).

The vita has been removed from the scanned document

MODEL ADHESIVE STUDIES USING BLOCK COPOLYMERS

by

Anne Booth Wood

(ABSTRACT)

The diversity of adhesive/adherend pairs has created innumerable unique combinations of thermodynamic, kinetic, chemical, physical and rheological contributions with which to explain adhesion processes. So complex are the interrelationships of these contributions to the overall composite system that little information can be extracted about the role of the adhesive properties themselves. This study attempts to simplify the number of variables influencing the strength of adhesive joints by employing a series of styrene-isoprene-styrene linear triblock copolymers as model hot-melt adhesives for titanium 6-4 alloy substrates. The block copolymer samples have narrow molecular weight distributions and styrene contents ranging from 20 to 60% by weight. For these systems a finite number of "dominant" variables are defined including 1) adherend wettability, 2) mechanical properties, 3) rheology, 4) adhesive and adherend contamination, and 5) temperature-pressure cycles for joint formation. Characterization of the block copolymer series in each of these areas is presented. Copolymer morphology emerges as an important variable affecting the material and adhesive properties of these systems.

The adhesive joints prepared from these samples are simple lap shear specimens. Comparative joint strengths and joint fracture

energies of the series of copolymer adhesives are rationalized in terms of styrene content, styrene domain connectivity and domain orientation. Scanning electron microscopy is employed to examine the surface characteristics of the fractured adhesives. Distinctive failure features are associated with the styrene content and dissipative capacities of the adhesives.